Mathematics

https://www.aimspress.com/journal/Math

AIMS Mathematics, 11(9): 30260–30279.
DOI: 10.3934/math.20261199
Received: 04 June 2026
Revised: 27 August 2026
Accepted: 14 September 2026
Published: 17 September 2026

Research article

Asymptotic analysis of soliton solutions of nonlinear Granular equation via WAS-Exp neural network technique

Waseem Razzaq[1], **Asim Zafar**[1], **Naif Almusallam**[2,*] **and Ahmed Al Nuaim**[2]

[1] Department of Mathematics, COMSATS University Islamabad, Vehari Campus, Pakistan
[2] Department of Management Information Systems, School of Business, King Faisal University, Al-Ahsa 31982, Saudi Arabia

* **Correspondence:** Email: nalmuslem@kfu.edu.sa.

Abstract: This paper presented an analytical method called the WAS-Exp neural network method to develop precise solutions of nonlinear evolution equations. The novelty of WAS-Exp lies in its unified neural-network formulation, in which an exponential-function mechanism is embedded directly into the solution construction rather than used as a separate ansatz. Consequently, distinct wave families can be derived systematically from a single framework, reducing the dependence on separately designed solution forms. In order to illustrate its efficacy, the technique was used on the pre-compressed one-dimensional Granular crystal equation, which formed a paradigm for the modeling of nonlinear wave propagation in dispersive media like the optical fibers and plasma channels. The application of the WAS-Exp neural network technique produced an extensive family of high-precision solutions of the analytic, unfolding nonlinear waves. Further, asymptotic analysis was employed on the solutions to check the x-asymptotic and t-asymptotic behavior of the solutions. Physical properties and propagation of these solutions were further illustrated by the use of two- and three-dimensional plots, which showed the diversity and stability of their structure. The findings revealed that the suggested approach was an efficient tool to study nonlinear systems with complex nature that could be used in the fields of physical sciences, fluid dynamics, and optical communications technologies.

Keywords: the WAS-Exp neural network method; pre-compressed one-dimensional Granular crystal model; solitons; asymptotic analysis
Mathematics Subject Classification: 35Q55, 35C08, 37K10, 35A20

1. Introduction

Research and technological advancement to depict real-world processes are carried out using nonlinear partial differential equations (NLPDEs). In this case the outputs of NLPDEs have grown in significance of study and analytical solutions [1]. A wide range of phenomena in biology, physics, economics, engineering, and some other domains are explained by NLPDEs, which are an important branch of mathematical models. NLPDEs show a complicated behavior when it comes to nonlinear terms. The main outcomes of these occurrences are shock waves, pattern development, and turbulence. NLPDE applications commonly include both numerical and theoretical elements. PDEs thoroughly investigate the qualitative behaviors of solutions, which include stability, uniqueness, and existence. The links among analytical and computational approaches are essential, as a researcher tries to explore and explain the complex dynamics that are formed by NLPDEs. Different methods and tools are used for the better understanding of the architecture of different physical phenomena [2]. Complicated wave phenomena in fields like fluid dynamics, chemistry, physics, and biology are widely used and explained by fractional counterparts and NLPDEs [3, 4].

An important and interesting topic of study for scientists is to hunt for the analytical solutions to NLPDEs. Researchers use advanced mathematical approaches to attain precise numerical solutions. These equations can be used to simulate a wide range of natural processes. Advancements in PDEs have allowed researchers to get solutions. The study and resolution of PDEs is critical to many physical processes. Many researchers have developed many mathematical tools and techniques to help them solve complex PDEs analytically. Significantly, in recent years many experts have shown interest in soliton theory. Solitons are thought to be suitable for fiber transmission systems because they function as natural optical data bits, dispersing over long distances with polarization mode and sensitivity to chromatic dispersion, and maintaining particle-like characteristics even in the face of turbulence [5, 6]. An experiment conducted in 1980 validated Hasegawa and Tappert's 1973 prediction of the presence of solitons in nonlinear optical fibers. Since then, theoretical and experimental physicists have gained interest in the subject due to its numerous potential applications. Optical solitons can be found in optical wave bulk materials, guides, photonic crystal fibers such as photo-refractive and photo-polymer materials, and other applications [7, 8]. Because of their extensive research in mathematical physics and telecommunication engineering, scientists and academics are very interested in solitons. Consequently, lone waves have been more crucial for resolving many kinds of nonlinear equations. These solutions and applications make it easier to comprehend the stability of physical systems and behavior [9]. Understanding physical events is made easier by the accessibility of precise solutions for a wide range of physical systems. These fixes are crucial since they lay the groundwork for additional research. To get an exact solution, a physical system's behavior must be described as an ODE or PDE. PDEs enable the simulation of complex industrial or natural events. Many scholars have developed a vast range of techniques to successfully address these problems. In past year various techniques have been widely acknowledged and are commonly used: the modified Sardar sub-equation technique [10], the WAS-Exp neural network technique [11], the Lie classical technique [12], the truncated Painlevé technique [13], the Unified technique [14], the Riccati equation mapping technique [15], the Adomian decomposition technique [16], the WAS-neural network technique [17], the Darboux transformation technique [18], the modified extended mapping method [19], the $(\frac{G'}{G})$-expansion technique [20], the F-expansion technique [21], and the Bilinear neural network method [22].

Many models have been employed to study the nonlinear systems, such as the Biswas-Arshed equation [23], the Kairat-II-X equation [24], the Kadomtsev-Petviashvili equation [25], the Boussinesq water wave equation [26], the Pochhammer–Chree equation [27], and many others. The pre-compressed one-dimensional granular crystal model [28] is defined as:

$$w_{tt} - c_0^2\, w_{xx} - 2c_0\, \gamma\, w_{xxxx} + \epsilon\, w_x\, w_{xx} = 0, \tag{1.1}$$

where $c_0^2 = 6R^2 d_0^{1/2}$, $c = \frac{c_0 R^2}{6}$, $\epsilon = \frac{c_0^2 R}{d_0}$, and x denotes the dimensionless spatial coordinate. Existing study on the one-dimensional granular crystal model presented in Table 1.

Table 1. Summary of existing studies on the one-dimensional granular crystal model.

References	Methodology	Summary of Work
[29]	Parameter estimation (Optimization method)	Investigated dissipative effects in one dimensional crystal model.
[30]	Newton–Krylov method	Provided a study of nonlinear coherent structures in one dimensional granular model.
[31]	Finite element method	Studied the solitary wave propagation in one dimensional granular model.
[32]	Generalized Riccati equation mapping method	Studied the exponential, trigonometry, and hyperbolic forms of solutions.
Present study	WAS-Exp neural network method	Derived including such as kink type and anti-kink type waveforms solutions, performed their asymptotic behavior of the solutions.

Recently a hot topic neural network has been widely discussed in the last decade. There are many neural network models and the techniques are developed in the different field of sciences and engineering. Complex valued zeroing neural network models have also been developed as effective computational frameworks for dynamic matrix inversion and other nonlinear engineering problems, with particular emphasis on convergence speed, robustness, and noise suppression [33]. Zeroing neural network (ZNN) models have emerged as effective dynamic-system solvers for time-varying mathematical and real-time control problems, offering improved convergence and robustness compared with conventional gradient based neural network approaches [34]. Event triggered adaptive dynamic programming has also been combined with critic neural networks to achieve robust optimal tracking control of uncertain nonlinear systems under input constraints and external disturbances [35]. Self-attention-enhanced physics-informed neural networks (SA-PINNs) have also been developed to improve the accuracy and physical interpretability of neural-network-based predictions by incorporating governing physical information into the learning process [36]. Physics-informed machine learning approaches have also been employed to incorporate physical constraints into data-driven models, improving the accuracy, physical consistency, and interpretability of predictions for complex engineering systems [37]. Localized wave structures such as gap solitons and truncated Bloch waves have also been investigated in nonlinear periodic media, where the interplay between linear and nonlinear lattice modulations plays a crucial role in their stability, formation, and propagation dynamics [38]. Due to the above challenges and gaps in research, the present study of the WAS-Exp neural network method, systematically builds precise solutions to nonlinear evolution equations. Under a single formulation, the approach produces a large array of wave solutions, such as solitary, hyperbolic, trigonometric, and rational structures, and hence its adaptability and strength. In this study, we apply the WAS-Exp neural network method on the pre-compressed granular crystal model and different types of solutions, which can make a further contribution to the further comprehension of nonlinear wave dynamics and their possible application to the contemporary physical sciences.

Objectives and main contributions

This study uses the WAS-Exp neural network method to create exact analytical solutions of the one-dimensional granular crystal model. The primary contributions of this work are as follows:

- The WAS-Exp neural network method will be used on the one-dimensional granular crystal model.
- To obtain various families of precise solutions, such as hyperbolic, trigonometric, and rational wave structures.
- To use graphical analysis to examine the nonlinear wave dynamics related to the obtained solutions.
- Apply the asymptotic analysis on the wave solutions to check x-asymptotic and t-asymptotic behavior .

This work consists of the following sections: Section 2 presents the description of the considered technique and its application. Section 3 consists of a graphical profile of the obtained solutions and discussion. Section 4 consists of the asymptotic analysis of the gained solutions. Section 5 includes a conclusion.

2. The WAS-Exp neural network technique

This section presents the description of the WAS-Exp neural network method [11]. This method is designed to obtain exact solutions of NLPDE of the general form:

$$H\left(w, w_x, w_t, w_{xx}, w_{xt}, w_{tt}, \dots\right) = 0. \tag{2.1}$$

Polynomial function $H(w)$ has $w_x = \frac{\partial w}{\partial x}$, $w_t = \frac{\partial w}{\partial t}$, and so on.

To determine exact solutions of Eq (2.1), we define a neural network-based proposed solution function (see Figure 1). The neural network output serves as the analytical solution. Specifically, the solution function is given by

$$w = \sum_{l_n \in L_n} \varrho_{l_n,w} \, F_{l_n}\left(\Theta_{l_n}\right), \tag{2.2}$$

where:

- $\varrho_{l_n,w}$ represents the weight associated with the connection between neuron l_n in the last hidden layer and the resultant neuron w.
- F represents in the neural network structure as the activation function.
- The indices associated with the neurons in the n-th layer represents as $L_n = \{l_{n-1}+1, l_{n-1}+2, \dots, l_n\}$.

The neural network includes two types of parameters:

- weights $\varrho_{i,j}$,
- bias terms ϑ_l,

which connect neuron i in one layer to neuron j in the next layer. The input to neuron l_i in the i-th layer is defined as

$$\Theta_{l_i} = \sum_{l_{i-1} \in L_{i-1}} \varrho_{l_{i-1},l_i} \, F_{l_{i-1}}\left(\Theta_{l_{i-1}}\right) + \vartheta_{l_i}, \quad i = 1, 2, \dots, n. \tag{2.3}$$

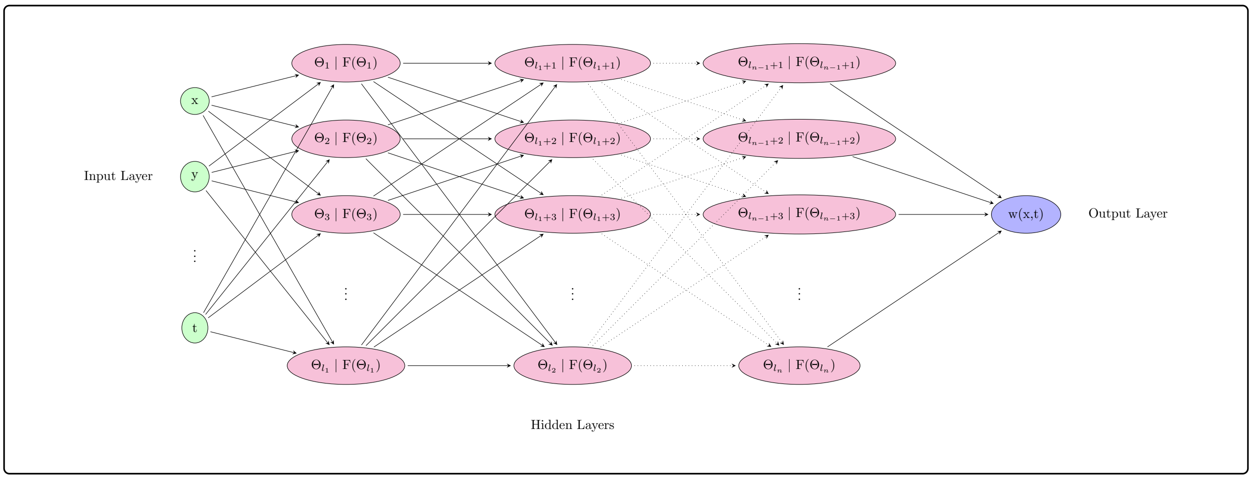

Figure 1. Neural networks model.

The WAS-Exp neural network technique utilizes the characteristics of the function $e^{-\psi(\Theta)}$, where $\psi(\Theta)$ satisfies the differential equation

$$\varphi'(\Theta) = -\left(\tau e^{-\varphi(\Theta)} + \eta e^{\varphi(\Theta)}\right). \tag{2.4}$$

The solutions of Eq (2.4) can be classified into several families:
Family 1: Hyperbolic function solutions (when $\tau\eta < 0$)

$$\varphi(\Theta) = \begin{cases} \ln\left(\sqrt{\frac{\tau}{-\eta}}\tanh\left(\sqrt{-\tau\eta}(\Theta + G)\right)\right), \\ \ln\left(\sqrt{\frac{\tau}{-\eta}}\coth\left(\sqrt{-\tau\eta}(\Theta + G)\right)\right). \end{cases} \tag{2.5}$$

Family 2: Trigonometric function solutions (when $\tau\eta > 0$)

$$\varphi(\Theta) = \begin{cases} \ln\left(\sqrt{\frac{\tau}{\eta}}\tan\left(\sqrt{\tau\eta}(\Theta + G)\right)\right), \\ \ln\left(\sqrt{\frac{\tau}{\eta}}\cot\left(\sqrt{\tau\eta}(\Theta + G)\right)\right). \end{cases} \tag{2.6}$$

Family 3: Rational function solution (when $\eta > 0$ and $\tau = 0$)

$$\varphi(\Theta) = \ln\left(\frac{1}{-\eta(\Theta + G)}\right). \tag{2.7}$$

Family 4: Logarithmic solution (when $\eta = 0$ and $\tau \neq 0$)

$$\varphi(\Theta) = \ln\left(\tau(\Theta + G)\right). \tag{2.8}$$

In the context, τ, η, and G represent are nonzero real-valued constants.
The suggested technique consists of two steps:

(1) Utilizing the analytical solutions of $e^{-\varphi(\Theta)}$ as activation functions within the neural network architecture.

(2) The constructed neural network is used to generate proposed solution functions, which reduce the NLPDE to an equivalent algebraic system that can be solved shows in the Figure 2.

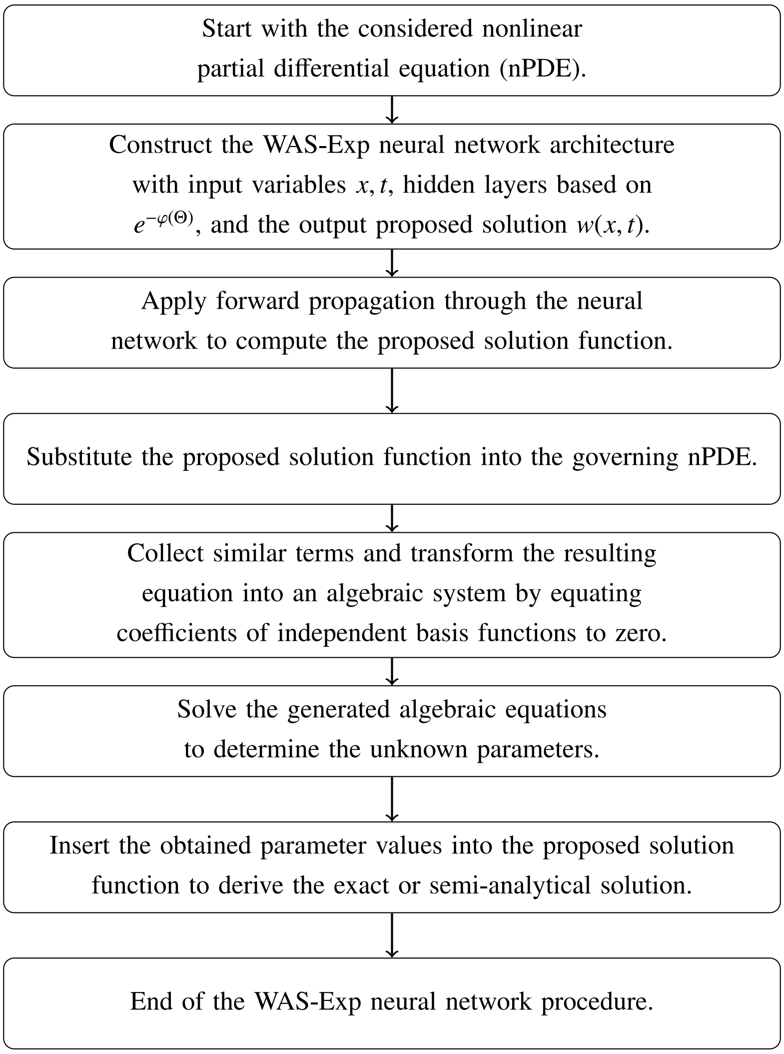

Figure 2. Flowchart representation of the WAS-Exp neural network methodology for solving NLPDEs.

2-2-2-1 neural network architecture

We utilize the double hidden layer architecture as shown in Figure 3.

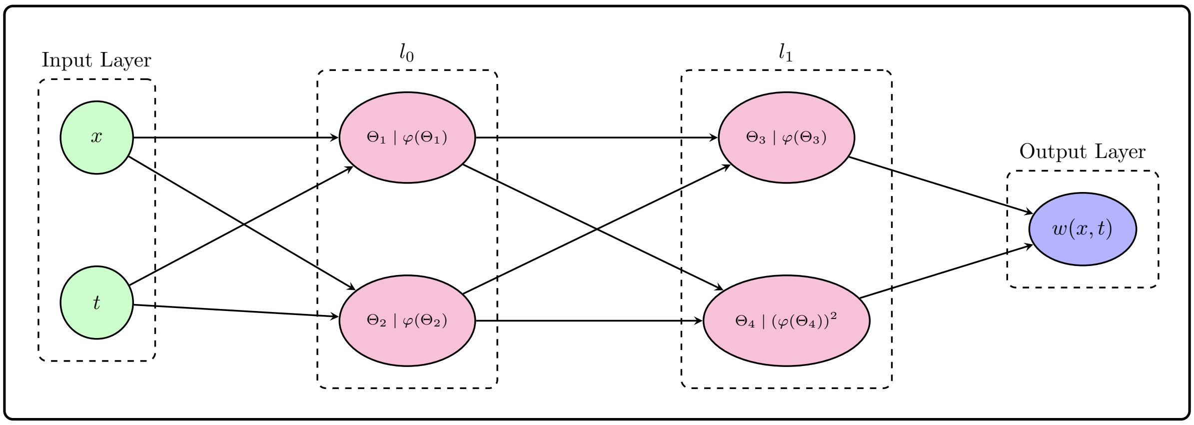

Figure 3. Double hidden layer model.

$$\begin{cases} \Theta_1 = x\varrho_{\{1,1\}} + t\varrho_{\{2,1\}} + b\vartheta_1, \\ \Theta_2 = x\varrho_{\{1,2\}} + t\varrho_{\{2,2\}} + \vartheta_2, \\ \Theta_3 = \varphi\left(\Theta_1\right)\varrho_{\{1,3\}} + \varphi\left(\Theta_2\right)\varrho_{\{2,3\}} + \vartheta_3, \\ \Theta_4 = \varphi\left(\Theta_1\right)\varrho_{\{1,4\}} + \varphi\left(\Theta_2\right)\varrho_{\{2,4\}} + \vartheta_4, \\ \Theta = F\left(\Theta_3\right)\varrho_{\{1,5\}} + F\left(\Theta_4\right)\varrho_{\{2,5\}} + \vartheta_5. \end{cases} \tag{2.9}$$

The proposed network structure takes the independent variables x and t as inputs, with the hidden layer utilizing the identity function $(\cdot)$ along with the quadratic function $(\cdot)^2$ as activation mechanisms. Hence, the output layer is given by

$$\begin{cases} \Theta_1 = x\varrho_{\{1,1\}} + t\varrho_{\{2,1\}} + \vartheta_1, \\ \Theta_2 = x\varrho_{\{1,2\}} + t\varrho_{\{2,2\}} + \vartheta_2, \\ \Theta_3 = \varphi\left(\Theta_1\right)\varrho_{\{1,3\}} + \varphi\left(\Theta_2\right)\varrho_{\{2,3\}} + \vartheta_3, \\ \Theta_4 = \varphi\left(\Theta_1\right)\varrho_{\{1,4\}} + \varphi\left(\Theta_2\right)\varrho_{\{2,4\}} + \vartheta_4, \\ w = \left(\Theta_3\right)\varrho_{\{1,5\}} + \left(\Theta_4\right)^2\varrho_{\{2,5\}} + \vartheta_5. \end{cases} \tag{2.10}$$

By substituting Eq (2.10) into Eq (1.1), we derive the following algebraic system of equations:

After solving the above system, we get the following solutions sets.

Set 1:

$$\gamma = -\frac{\epsilon\varrho_{\{1,5\}}\varrho_{\{2,3\}}}{24c_0\eta\varrho_{\{1,2\}}}, \quad \varrho_{\{2,2\}} = \frac{\varrho_{\{1,2\}}\sqrt{\tau\epsilon\varrho_{\{1,2\}}\varrho_{\{1,5\}}\varrho_{\{2,3\}} + 3c_0^2}}{\sqrt{3}}, \quad \varrho_{\{1,3\}} = 0, \quad \varrho_{\{2,5\}} = 0. \tag{2.11}$$

Family 1: Hyperbolic function solutions (when $\tau\beta < 0$)

$$w(x,t) = \varrho_{\{1,5\}}\left(\sqrt{-\tfrac{\tau}{\eta}}\varrho_{\{2,3\}}\tanh\left(\sqrt{-\eta\tau}\left(\frac{t\varrho_{\{1,2\}}\sqrt{\tau\epsilon\varrho_{\{1,2\}}\varrho_{\{1,5\}}\varrho_{\{2,3\}}+3c_0^2}}{\sqrt{3}} + x\varrho_{\{1,2\}} + G + \vartheta_2\right)\right) + \vartheta_3\right) + \vartheta_5, \tag{2.12}$$

$$w(x,t) = \varrho_{\{1,5\}}\left(\sqrt{-\frac{\tau}{\eta}}\varrho_{\{2,3\}}\coth\left(\sqrt{-\eta\tau}\left(\frac{t\varrho_{\{1,2\}}\sqrt{\tau\epsilon\varrho_{\{1,2\}}\varrho_{\{1,5\}}\varrho_{\{2,3\}}+3c_0^2}}{\sqrt{3}}+x\varrho_{\{1,2\}}+G+\vartheta_2\right)\right)+\vartheta_3\right)+\vartheta_5. \tag{2.13}$$

Set 2:

$$\varrho_{\{1,3\}} = 0,\ \varrho_{\{1,4\}} = 0,\ \varrho_{\{2,4\}} = 0,\ \gamma = -\frac{\epsilon\varrho_{\{1,5\}}\varrho_{\{2,3\}}}{24c_0\eta\varrho_{\{1,2\}}},\ \varrho_{\{2,2\}} = \frac{\varrho_{\{1,2\}}\sqrt{\tau\epsilon\varrho_{\{1,2\}}\varrho_{\{1,5\}}\varrho_{\{2,3\}}+3c_0^2}}{\sqrt{3}}. \tag{2.14}$$

Family 1: Hyperbolic function solutions (when $\tau\beta < 0$)

$$w(x,t) = \varrho_{\{1,5\}}\left(\sqrt{-\frac{\tau}{\eta}}\varrho_{\{2,3\}}\tanh\left(\sqrt{-\eta\tau}\left(\frac{t\varrho_{\{1,2\}}\sqrt{\tau\epsilon\varrho_{\{1,2\}}\varrho_{\{1,5\}}\varrho_{\{2,3\}}+3c_0^2}}{\sqrt{3}}+x\varrho_{\{1,2\}}+G+\vartheta_2\right)\right)+\vartheta_3\right)+\vartheta_4^2\varrho_{\{2,5\}}+\vartheta_5, \tag{2.15}$$

$$w(x,t) = \varrho_{\{1,5\}}\left(\sqrt{-\frac{\tau}{\eta}}\varrho_{\{2,3\}}\coth\left(\sqrt{-\eta\tau}\left(\frac{t\varrho_{\{1,2\}}\sqrt{\tau\epsilon\varrho_{\{1,2\}}\varrho_{\{1,5\}}\varrho_{\{2,3\}}+3c_0^2}}{\sqrt{3}}+x\varrho_{\{1,2\}}+G+\vartheta_2\right)\right)+\vartheta_3\right)+\vartheta_4^2\varrho_{\{2,5\}}+\vartheta_5. \tag{2.16}$$

3. Graphical profile of solutions

Graphical profile of the obtained solutions are illustrated in this section. Choosing the suitable values of the present different parameters in the obtained solutions help out the to represent the kink and anti-kink profile of the solutions. By choosing values of parameters as $\vartheta_2 = 1.7, \vartheta_3 = 0.1, \vartheta_5 = 0, \varrho_{\{2,3\}} = 0.3, \tau = -1, \eta = 0.5, G = 0.7, \varrho_{\{1,2\}} = 0.3, \varrho_{\{1,5\}} = 0.6, c_0 = 0.9, \epsilon = 0.5$, with domain $x \in [-15, 15]$ and $t \in [-25, 25]$, the wave profile is shown in the Figure 4. Setting the parameter's values to $\vartheta_2 = -1.7, \vartheta_3 = -0.1, \vartheta_5 = 0, \varrho_{\{1,2\}} = -0.3, \tau = -1, \eta = 0.5, G = 0.7, \varrho_{\{2,3\}} = 0.3, \varrho_{\{1,5\}} = 0.6, c_0 = 0.9, \epsilon = 0.5$, with domain $x \in [-5, 5]$ and $t \in [-25, 25]$, the wave profile is shown in the Figure 5. Setting the parameter's values to $\vartheta_2 = 0.3, \vartheta_3 = 0.3, \vartheta_4 = 0.4, \vartheta_5 = 0.5, \varrho_{\{2,3\}} = 0.3, \varrho_{\{2,5\}} = 0.6, \tau = -1, \eta = 0.5, G = 0.4, \varrho_{\{1,2\}} = 1.3, \varrho_{\{1,5\}} = 1.6, c_0 = 0.9, \epsilon = 0.3$, with domain $x \in [-5, 5]$ and $t \in [-25, 25]$, the wave profile is shown in the Figure 6.

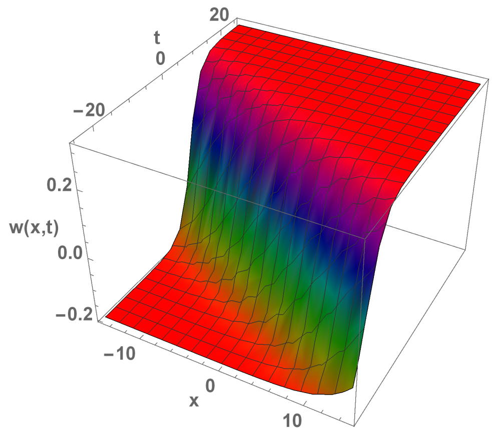

(a)

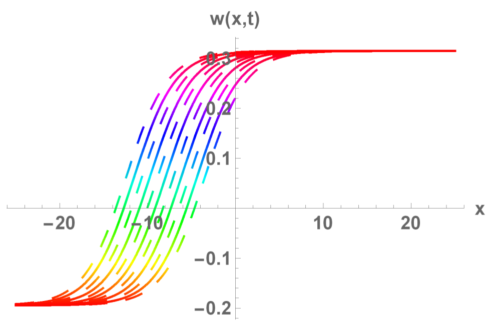

(b)

Figure 4. The graphical representation of the anti-kink wave profile corresponding to the solution is shown in Eq (2.12).

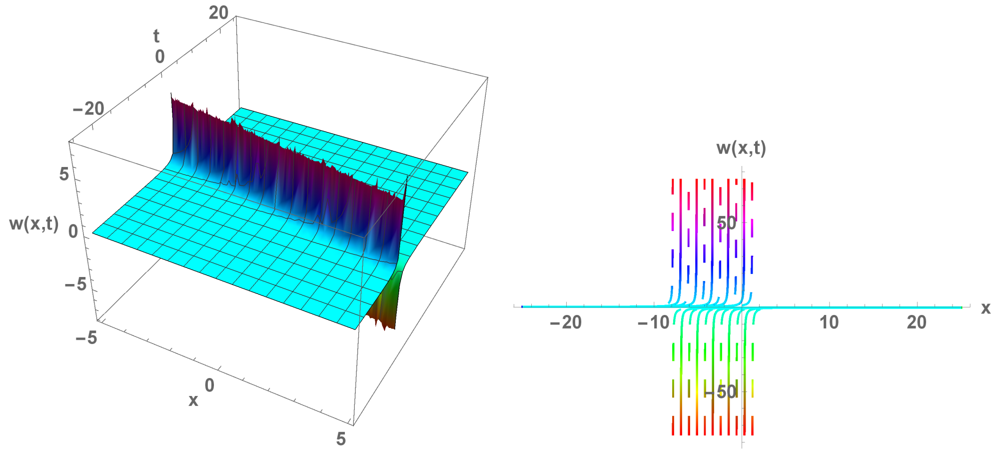

(a) (b)

Figure 5. The graphical representation of the kink wave profile corresponding to the solution is shown in Eq (2.13).

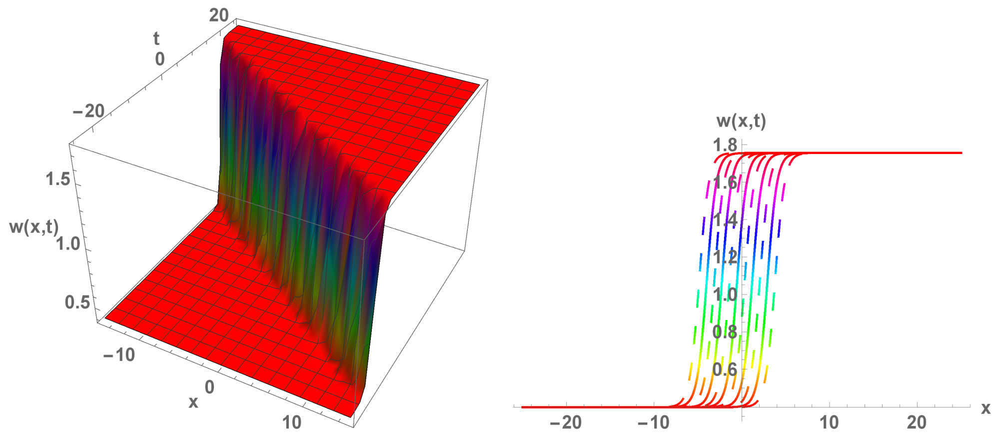

(a) (b)

Figure 6. The graphical representation of the kink wave profile corresponding to the solution is shown in Eq (2.15).

4. Results and discussion

This portion consist of the results and discussion on the obtained solutions via comparing with the other solution of the considered model. Several studies have been reported on the one-dimensional granular crystal model using different analytical and numerical approaches. In [29], the parameter estimation method was employed to investigate the effects of dissipation in the one-dimensional crystal model. The Newton-Krylov method was used in [30] to study nonlinear coherent structures in the one-dimensional granular model, while the finite element method was adopted in [31] to investigate solitary wave propagation. Furthermore, [32] employed the generalized Riccati equation mapping method to derive exponential, trigonometric, and hyperbolic forms of solutions. In contrast to these existing studies, the present work employs the WAS-Exp neural network method to derive various wave structures, including kink type, anti-kink type, and singular type solutions, for the one-dimensional granular crystal model. In addition, the asymptotic behavior of the obtained solutions are investigated, providing further insight into their qualitative properties and distinguishing the present study from the previously reported results.

Table 2 presents the comparison between the existing and new results.

Table 2. Comparison of the present study with the existing literature.

Feature	Previous study	Present study
Need travelling wave transformation	✓	×
Balance method	✓	×
Hyperbolic solutions	✓	✓
Solitary solutions	×	✓
Kink/Anti-kink wave solutions	×	✓
Asymptotic analysis	×	✓
2D and 3D graphical illustrations	✓	✓

5. Asymptotic analysis

This section presents the asymptotic analysis of the obtained solutions in order to investigate their behavior under limiting conditions and to examine their physical characteristics at infinity [39]. To obtain a clearer understanding of the long-time evolution and dynamical characteristics of the solution $w(x,t)$ presented in Eq (2.12), an asymptotic analysis is carried out to examine the behavior of the solution under limiting conditions.

x-asymptotic as $x \to \pm\infty$ at $t = 0$

For the case when time $t = 0$, the given solution reduces to

$$w(x,0) = \varrho_{\{1,5\}}\left(\sqrt{-\frac{\tau}{\eta}}\varrho_{\{2,3\}} \tanh\left(\sqrt{-\eta\tau}\,(x\varrho_{\{1,2\}} + G + \vartheta_2)\right) + \vartheta_3\right) + \vartheta_5.$$

Figure 7 shows the limits $x \to \pm\infty$, and the hyperbolic tangent term approaches ±1, respectively. Consequently, the solution approaches two finite asymptotic levels, whose difference characterizes the amplitude of the spatial transition. This confirms the bounded and kink-type nature of the wave and indicates that the granular medium tends toward distinct equilibrium states on either side of the localized transition region.

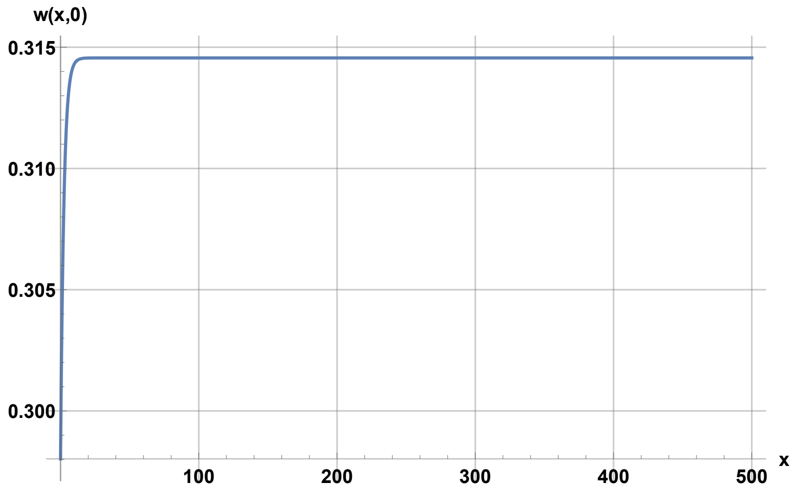

Figure 7. x-asymptotic analysis of the solution shown in Eq (2.12).

t-asymptotic as $t \longrightarrow \pm\infty$ at $x = 0$

For the case when $x = 0$, the solution takes the form

$$w(0,t) = \varrho_{\{1,5\}}\left(\sqrt{-\frac{\tau}{\eta}}\varrho_{\{2,3\}}\tanh\left(\sqrt{-\eta\tau}\left(\frac{t\varrho_{\{1,2\}}\sqrt{\tau\epsilon\varrho_{\{1,2\}}\varrho_{\{1,5\}}\varrho_{\{2,3\}}+3c_0^2}}{\sqrt{3}}+G+\vartheta_2\right)\right)+\vartheta_3\right)+\vartheta_5.$$

In particular, Figure 8 shows $\tanh(\xi) \longrightarrow \pm 1$ as $\xi \longrightarrow \pm\infty$, the asymptotic values of $w(0,t)$ are determined by the constant terms and the amplitude factor in Eq (2.12). Hence, the asymptotic analysis confirms the existence of two finite limiting states and characterizes the transition amplitude of the kink-type structure. Similarly to obtain a clearer understanding of the long-time evolution and dynamical characteristics of the solution $w(x,t)$ presented in Eq (2.13), an asymptotic analysis is carried out to examine the behavior of the solution under limiting conditions.

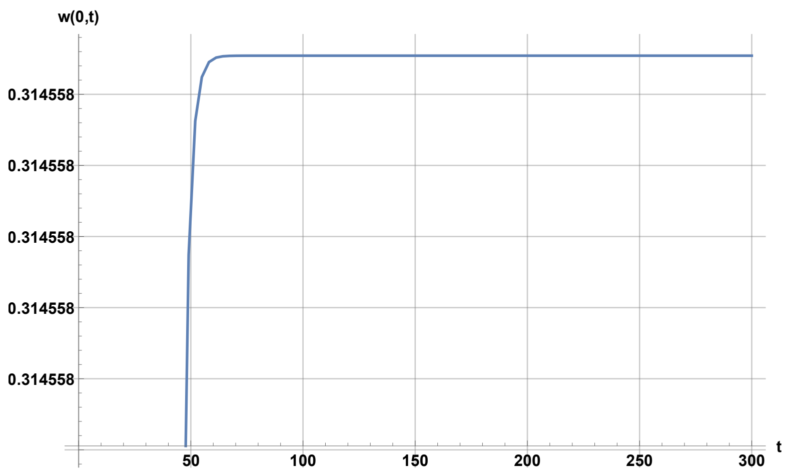

Figure 8. t-asymptotic analysis of the solution shown in Eq (2.12).

x-asymptotic as $x \to \pm\infty$ at $t = 0$

For the case when time $t = 0$, the given solution reduces to

$$w(x,0) = \varrho_{\{1,5\}}\left(\sqrt{-\frac{\tau}{\eta}}\varrho_{\{2,3\}}\coth\left(\sqrt{-\eta\tau}\left(x\varrho_{\{1,2\}} + G + \vartheta_2\right)\right) + \vartheta_3\right) + \vartheta_5.$$

Figure 9 shows x-asymptotic for the Eq (2.13).

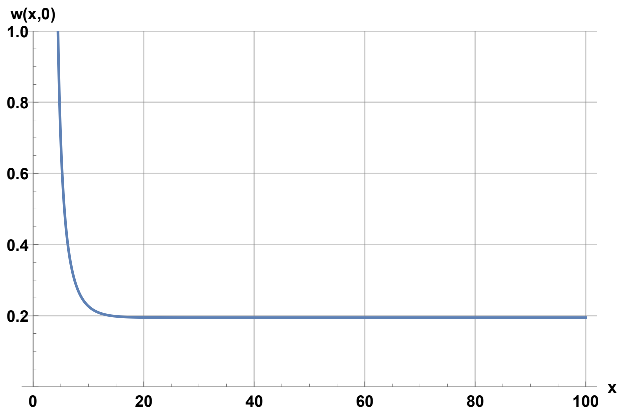

Figure 9. x-asymptotic analysis of the solution shown in Eq (2.13).

t-asymptotic as $t \to \pm\infty$ at $x = 0$

For the case when $x = 0$, the given solution takes the form

$$w(0,t) = \varrho_{\{1,5\}}\left(\sqrt{-\frac{\tau}{\eta}}\varrho_{\{2,3\}}\coth\left(\sqrt{-\eta\tau}\left(\frac{t\varrho_{\{1,2\}}\sqrt{\tau\epsilon\varrho_{\{1,2\}}\varrho_{\{1,5\}}\varrho_{\{2,3\}} + 3c_0^2}}{\sqrt{3}} + G + \vartheta_2\right)\right) + \vartheta_3\right) + \vartheta_5.$$

Figure 10 shows y-asymptotic for the Eq (2.13).

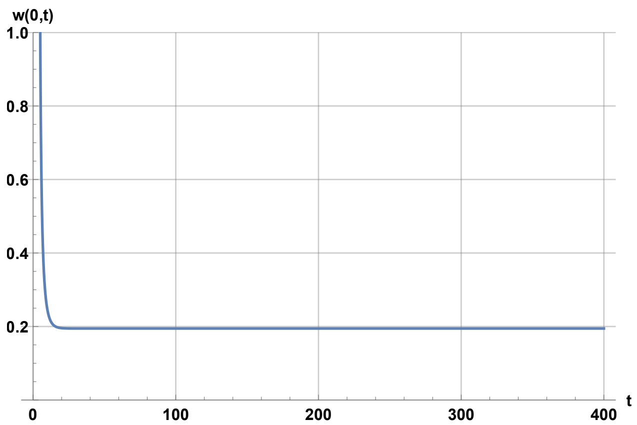

Figure 10. t-asymptotic analysis of the solution shown in Eq (2.13).

6. Conclusions

Nonlinear wave dynamics in a pre-compressed one-dimensional Granular equation have been successfully investigated in this work by using the WAS-Exp neural network method obtained by the hyperbolic solutions. The visualizations provided in the graphical analysis, specifically the two- and three-dimensional ones, demonstrate the kink type, singular type, and anti-kink type variety of the obtained wave structures. Furthermore, asymptotic analysis is employed on the solutions to check the x-asymptotic and t-asymptotic behavior of the solutions. In general, the findings validate the fact that the suggested approach is sound, systematic, and quite useful in the resolution of nonlinear evolution equations. In addition to the particular model discussed in this research, the WAS-Exp neural network approach has a great potential of being extended to other complex nonlinear systems that occur in the study of plasma physics, optical fibers, fluid dynamics, and many more. It thus presents new possibilities to the analysis of nonlinear phenomena and offers a useful resource to theory and practical studies in the future.

Author contributions

Waseem Razzaq, Asim Zafar: Concept, Methodology, Investigation, Writing – review and editing. Naif Almusallam, Ahmed Al Nuaim: Formal analysis, Resources, Visualization, Writing – review and editing. All authors have read and approved the final version of the manuscript for publication.

Use of Generative-AI tools declaration

The authors declares they have not used Artificial Intelligence (AI) tools in the creation of this article.

Acknowledgments

This work was funded by the Deanship of Scientific Research, Vice Presidency for Graduate Studies and Scientific Research, King Faisal University, Saudi Arabia [Grant No. KFU263879].

Conflict of interest

There is no conflict of interest all authors agreed.

References

1. M. M. A. Khater, B. Ghanbari, K. S. Nisar, D. Kumar, Novel exact solutions of the fractional Bogoyavlensky-Konopelchenko equation involving the Atangana-Baleanu-Riemann derivative, *Alex. Eng. J.*, **59** (2020), 2957–2967. https://doi.org/10.1016/j.aej.2020.03.032
2. H. M. Ali, A. S. Ali, M. Mahmoud, A. H. Abdel-Aty, Analytical approximate solutions of fractional nonlinear Drinfeld–Sokolov-Wilson model using modified Mittag-Leffler function, *J. Ocean Eng. Sci.*, 2022. https://doi.org/10.1016/j.joes.2022.06.006

3. A. Zafar, M. Raheel, M. R. Ali, Z. Myrzakulova, A. Bekir, R. Myrzakulov, Exact solutions of M-fractional Kuralay equation via three analytical schemes, *Symmetry*, **15** (2023), 1862. https://doi.org/10.3390/sym15101862
4. K. Yesmakhanova, Z. Myrzakulova, R. Myrzakulov, G. Nugmanova, Soliton surfaces induced by the Kuralay, Kairat and Akbota equations, *15th Symposium on Integrable Systems*, Bialystok, Poland, 2023. https://doi.org/10.13140/RG.2.2.16410.41928
5. W. A. Faridi, M. A. Bakar, Z. Myrzakulova, R. Myrzakulov, A. Akgül, S. M. El Din, The formation of solitary wave solutions and their propagation for Kuralay equation, *Results Phys.*, **52** (2023), 106774. https://doi.org/10.1016/j.rinp.2023.106774
6. M. Arshad, Y. Li, F. Yasin, K. Basheer, M. Sesay, Dynamics and stability of solitons in the higher-order dispersive cubic-quintic nonlinear Schrödinger equation: conservation laws and applications, *Discover Appl. Sci.*, **8** (2026), 7. https://doi.org/10.1007/s42452-025-08105-8
7. H. Y. Kong, R. Guo, Dynamic behaviors of novel nonlinear wave solutions for the Akbota equation, *Optik*, **282** (2023), 170863. https://doi.org/10.1016/j.ijleo.2023.170863
8. U. Demirbilek, V. Ala, K. R. Mamedov, Exact solutions of conformable time fractional Zoomeron equation via IBSEFM, *Appl. Math.-J. Chin. Univ.*, **36** (2021), 554–563. https://doi.org/10.1007/s11766-021-4145-3
9. B. Hong, J. Wang, Exact solutions for the generalized Atangana–Baleanu–Riemann fractional (3 + 1)-dimensional Kadomtsev–Petviashvili equation, *Symmetry*, **15** (2023), 3. https://doi.org/10.3390/sym15010003
10. S. Parveen, M. Abbas, T. Nazir, M. N. Anwar, M. R. Alharthi, M. Z. Yousaf, et al., Bifurcation analysis and soliton solutions of the generalized third-order nonlinear Schrödinger equation using two analytical approaches, *Sci. Rep.*, **16** (2026), 7065 https://doi.org/10.1038/s41598-026-37836-w
11. W. Razzaq, A. Zafar, A. Al Nuaim, N. Almusallam, Soliton wave phenomena of the complex hyperbolic nonlinear Schrödinger equation via emerging WAS-Exp neural network method and qualitative analysis, *AIMS Math.*, **10** (2025), 30806–30827. https://doi.org/10.3934/math.20251352
12. D. Chou, I. Iqbal, H. U. Rehman, O. H. Khalil, M. S. Osman, Heat conduction dynamics: a study of Lie symmetry, solitons, and modulation instability. *Rend. Fis. Acc. Lincei*, **36** (2025), 315–336. https://doi.org/10.1007/s12210-025-01302-y
13. M. Iqbal, M. Abbas, T. Nazir, W. F. Alfwzan, A. Birhanu, H. Ahmad, Dromion solutions for system of ion sound and Langmuir waves using truncated Painlevé approach, *Sci. Rep.*, **15** (2025), 37233. https://doi.org/10.1038/s41598-025-21049-8
14. R. Kumar, S. K. Mishra, Assessing the impact of heat vulnerability on urban public spaces using a fuzzy-based unified computational technique, *AI Soc.*, **40** (2025), 787–804. https://doi.org/10.1007/s00146-024-01904-4
15. M. A. S. Murad, U. Younas, H. Emadifar, M. Iqbal, W. W. Mohammed, K. K. Ahmed, Diverse soliton solutions to the conformable Ivancevic option pricing model via the modified generalized Riccati equation mapping method, *Math. Comput. Simul.*, **244** (2026), 213–225. https://doi.org/10.1016/j.matcom.2025.12.022

16. X. Song, Q. Gu, L. Wang, Application of the Fourier transform Adomian decomposition method for initial value problems, *Eng. Comput.*, **43** (2026), 1594–1623. https://doi.org/10.1108/EC-02-2025-0190

17. W. Razzaq, A. Zafar, Stability analysis of soliton solutions for the Kairat-X equation via a newly proposed WAS neural network method, *Z. Angew. Math. Phys.*, **77** (2026), 13. https://doi.org/10.1007/s00033-025-02659-8

18. S. Zhang, Y. Zhang, B. Xu, X. Li, Darboux and generalized Darboux transformations for the fractional integrable derivative nonlinear Schrödinger equation, *Int. J. Geom. Methods Mod. Phys.*, **23** (2026), 2440028. https://doi.org/10.1142/S0219887824400280

19. H. H. Hussein, H. M. Ahmed, S. A. Kandil, W. Alexan, Unveiling diverse solitons in the quintic perturbed Gerdjikov–Ivanov model via a modified extended mapping method, *Sci. Rep.*, **15** (2025), 15881. https://doi.org/10.1038/s41598-025-97981-6

20. A. Kaur, S. Saini, R. Budhiraja, Lie symmetry analysis, exact traveling wave solutions by $\left(\frac{G'}{G}\right)$-expansion method and qualitative analysis of Hirota–Schrödinger equation, *Commun. Math. Appl.*, **16** (2025), 451–461. https://doi.org/10.26713/cma.v16i2.3193

21. W. Razzaq, A. Zafar, A. Nazir, H. Ahmad, A. A. Zaagan, Dark, bright and singular optical solitons for Biswas–Milovic equation with Kerr and dual power law nonlinearities, *Mod. Phys. Lett. B*, **39** (2025), 2450443. https://doi.org/10.1142/S0217984924504438

22. H. H. Hussein, H. Mekawey, A. Elsheikh, Exact soliton, lump, and breather solutions of the $(3+1)$-dimensional Jimbo–Miwa equation via the bilinear neural network method, *Sci. Rep.*, **16** (2026), 11617. https://doi.org/10.1038/s41598-026-41485-4

23. A. Zafar, W. Razzaq, A. Nazir, M. A. Alomair, A. S. Al Naim, A. Alomair, Bifurcation analysis and solitons dynamics of the fractional Biswas–Arshed equation via analytical method, *Mathematics*, **13** (2025), 3147. https://doi.org/10.3390/math13193147

24. U. Demirbilek, A. H. Tedjani, A. R. Seadawy, Analytical solutions of the combined Kairat-II-X equation: a dynamical perspective on bifurcation, chaos, energy, and sensitivity, *AIMS Math.*, **10** (2025), 13664–13691. https://doi.org/10.3934/math.2025615

25. S. Zhang, G. Zhu, W. Huang, H. Wang, C. Yang, Y. Lin, Symbolic computation of analytical solutions for nonlinear partial differential equations based on bilinear neural network method, *Nonlinear Dyn.*, **113** (2025), 7121–7137. https://doi.org/10.1007/s11071-024-10715-7

26. W. Razzaq, A. Zafar, A. Nazir, M. U. D. Junjua, F. A. Awwad, E. A. Ismail, Optical soliton solutions of nonlinear differential Boussinesq water wave equation via two analytical techniques, *Results Phys.*, **64** (2024), 107898. https://doi.org/10.1016/j.rinp.2024.107898

27. M. M. A. Khater, Nonlinear effects in quantum field theory: applications of the Pochhammer–Chree equation, *Mod. Phys. Lett. B*, **39** (2025), 2550070, https://doi.org/10.1142/S0217984925500708

28. Z. G. Liu, J. Zhang, Y. S. Wang, G. Huang, Analytical solutions of solitary waves and their collision stability in a pre-compressed one-dimensional granular crystal, *Nonlinear Dyn.*, **104** (2021), 4293–4309. https://doi.org/10.1007/s11071-021-06534-9

29. R. Carretero-González, D. Khatri, M. A. Porter, P. G. Kevrekidis, C. Daraio, Dissipative solitary waves in granular crystals, *Phys. Rev. Lett.*, **102** (2009), 024102. https://doi.org/10.1103/PhysRevLett.102.024102

30. C. Chong, M. A. Porter, P. G. Kevrekidis, C. Daraio, Nonlinear coherent structures in granular crystals, *J. Phys.: Condens. Matter*, **29** (2017), 413003. https://doi.org/10.1088/1361-648X/aa7672

31. W. Zhang, J. Xu, Toward understanding solitary wave propagation in composite-cylinders-based 1D granular crystals, *Extreme Mech. Lett.*, **43** (2021), 101156. https://doi.org/10.1016/j.eml.2020.101156

32. Beenish, M. ur Rahman, D. Baleanu, Soliton formation and chaos dynamics in a one-dimensional pre-compressed granular crystal, *Ain Shams Eng. J.*, **17** (2026), 104080. https://doi.org/10.1016/j.asej.2026.104080

33. J. Jin, J. Zhu, L. Zhou, C. Chen, L. Wu, M. Lu, et al., A complex-valued variant-parameter robust zeroing neural network model and its applications, *IEEE Trans. Emerging Top. Comput. Intell.*, **8** (2024), 1303–1321. https://doi.org/10.1109/TETCI.2024.3356163

34. S. Cao, J. Jin, D. Zhang, C. Chen, A review of zeroing neural network: theory, algorithm and application, *Neurocomputing*, **643** (2025), 130425. https://doi.org/10.1016/j.neucom.2025.130425

35. B. Wang, J. Sun, B. Peng, X. Cui, L. Cheng, X. Zheng, Optimal event-triggered neural learning tracking control for pneumatic muscle antagonistic joint with asymmetric constraints, *IEEE Trans. Ind. Electron.*, **72** (2025), 14677–14687. https://doi.org/10.1109/TIE.2025.3585055

36. Y. Wang, Y. Li, S. Zhu, R. Gu, X. Shu, Z. Fan, et al., SA-PINN: a self-attention enhanced physics-informed neural network for multiaxial fatigue life prediction with small samples, *Adv. Eng. Softw.*, **216** (2026), 104124. https://doi.org/10.1016/j.advengsoft.2026.104124

37. Q. Nie, J. Zhang, Y. Wang, D. Wang, Q. Wang, Y. Shi, et al., Physics-informed machine learning for predicting stress wave transmission across realistic rock joints, *IEEE Access*, **13** (2025), 212735-212744. https://doi.org/10.1109/ACCESS.2025.3635734

38. J. Shi, Y. Chen, X. Pang, M. R. Belić, D. Mihalache, Y. Liu, et al., Gap solitons and truncated nonlinear Bloch waves in combined linear and quintic nonlinear lattices, *Opt. Express*, **34** (2026), 15864–15876. https://doi.org/10.1364/OE.587649

39. W. Razzaq, A. Zafar, A. Almusallam, F. K. Alarfaj, Asymptotic behavior of soliton solutions of the Kairat-X model via the Hirota bilinear method: Painlevé integrability and machine learning analysis, *AIMS Math.*, **10** (2025), 30029–30052. https://doi.org/10.3934/math.20251320

Appendix

$$
\begin{aligned}
&-32\gamma c_0\eta^3\tau\varrho_{\{1,4\}}^2\varrho_{\{2,5\}}\varrho_{\{1,1\}}^4-32\gamma c_0\eta^3\tau\varrho_{\{1,2\}}\varrho_{\{1,4\}}\varrho_{\{2,4\}}\varrho_{\{2,5\}}\varrho_{\{1,1\}}^3-32\gamma c_0\eta^3\tau\varrho_{\{1,2\}}^3\varrho_{\{1,4\}}\varrho_{\{2,4\}}\varrho_{\{2,5\}}\varrho_{\{1,1\}}\\
&-32\gamma c_0\eta^3\tau\varrho_{\{1,2\}}^4\varrho_{\{2,4\}}^2\varrho_{\{2,5\}}-2c_0^2\eta^2\varrho_{\{1,4\}}^2\varrho_{\{2,5\}}\varrho_{\{1,1\}}^2-4c_0^2\eta^2\varrho_{\{1,2\}}\varrho_{\{1,4\}}\varrho_{\{2,4\}}\varrho_{\{2,5\}}\varrho_{\{1,1\}}\\
&-2c_0^2\eta^2\varrho_{\{1,2\}}^2\varrho_{\{2,4\}}^2\varrho_{\{2,5\}}+2\eta^2\varrho_{\{1,4\}}^2\varrho_{\{2,1\}}^2\varrho_{\{2,5\}}+2\eta^2\varrho_{\{2,2\}}^2\varrho_{\{2,4\}}^2\varrho_{\{2,5\}}+4\eta^2\varrho_{\{1,4\}}\varrho_{\{2,1\}}\varrho_{\{2,2\}}\varrho_{\{2,4\}}\varrho_{\{2,5\}}\\
&-4\eta^3\epsilon\vartheta_4\varrho_{\{1,4\}}^3\varrho_{\{2,5\}}^2\varrho_{\{1,1\}}^3-12\eta^3\epsilon\vartheta_4\varrho_{\{1,2\}}\varrho_{\{1,4\}}^2\varrho_{\{2,4\}}\varrho_{\{2,5\}}^2\varrho_{\{1,1\}}^2-12\eta^3\epsilon\vartheta_4\varrho_{\{1,2\}}^2\varrho_{\{1,4\}}\varrho_{\{2,4\}}^2\varrho_{\{2,5\}}^2\varrho_{\{1,1\}}
\end{aligned}
$$

$$
\begin{aligned}
&-4\eta^3\epsilon\vartheta_4\varrho^3_{\{1,2\}}\varrho^3_{\{2,4\}}\varrho^2_{\{2,5\}} - 2\eta^3\epsilon\varrho_{\{1,3\}}\varrho^2_{\{1,4\}}\varrho_{\{1,5\}}\varrho_{\{2,5\}}\varrho^3_{\{1,1\}} - 2\eta^3\epsilon\varrho_{\{1,2\}}\varrho^2_{\{1,4\}}\varrho_{\{1,5\}}\varrho_{\{2,3\}}\varrho_{\{2,5\}}\varrho^2_{\{1,1\}}\\
&-4\eta^3\epsilon\varrho_{\{1,2\}}\varrho_{\{1,3\}}\varrho_{\{1,4\}}\varrho_{\{1,5\}}\varrho_{\{2,4\}}\varrho_{\{2,5\}}\varrho^2_{\{1,1\}} - 2\eta^3\epsilon\varrho^2_{\{1,2\}}\varrho_{\{1,3\}}\varrho_{\{1,5\}}\varrho^2_{\{2,4\}}\varrho_{\{2,5\}}\varrho_{\{1,1\}}\\
&-4\eta^3\epsilon\varrho^2_{\{1,2\}}\varrho_{\{1,4\}}\varrho_{\{1,5\}}\varrho_{\{2,3\}}\varrho_{\{2,4\}}\varrho_{\{2,5\}}\varrho_{\{1,1\}} - 2\eta^3\epsilon\varrho^3_{\{1,2\}}\varrho_{\{1,5\}}\varrho_{\{2,3\}}\varrho^2_{\{2,4\}}\varrho_{\{2,5\}} = 0,\\
&-12\tau^3\epsilon\varrho^3_{\{1,1\}}\varrho^4_{\{1,4\}}\varrho^2_{\{2,5\}} = 0,\\
&-20\tau^3\epsilon\varrho^3_{\{1,2\}}\varrho_{\{1,4\}}\varrho^3_{\{2,4\}}\varrho^2_{\{2,5\}} = 0,\\
&-12\tau^3\epsilon\varrho^3_{\{1,2\}}\varrho^4_{\{2,4\}}\varrho^2_{\{2,5\}} = 0,\\
&-96\gamma c_0\tau^4\varrho_{\{1,4\}}\varrho_{\{2,4\}}\varrho_{\{2,5\}}\varrho^4_{\{1,1\}} - 16\tau^3\epsilon\vartheta_4\varrho^2_{\{1,4\}}\varrho_{\{2,4\}}\varrho^2_{\{2,5\}}\varrho^3_{\{1,1\}} - 8\tau^3\epsilon\varrho_{\{1,3\}}\varrho_{\{1,4\}}\varrho_{\{1,5\}}\varrho_{\{2,4\}}\varrho_{\{2,5\}}\varrho^3_{\{1,1\}} = 0,\\
&-480\gamma c_0\eta\tau^3\varrho^2_{\{1,4\}}\varrho_{\{2,5\}}\varrho^4_{\{1,1\}} - 96\gamma c_0\eta\tau^3\varrho_{\{1,2\}}\varrho_{\{1,4\}}\varrho_{\{2,4\}}\varrho_{\{2,5\}}\varrho^3_{\{1,1\}} - 6c_0^2\tau^2\varrho^2_{\{1,4\}}\varrho_{\{2,5\}}\varrho^2_{\{1,1\}}\\
&-44\eta\tau^2\epsilon\vartheta_4\varrho^3_{\{1,4\}}\varrho^2_{\{2,5\}}\varrho^3_{\{1,1\}} - 28\eta\tau^2\epsilon\vartheta_4\varrho_{\{1,2\}}\varrho^2_{\{1,4\}}\varrho_{\{2,4\}}\varrho^2_{\{2,5\}}\varrho^2_{\{1,1\}} - 22\eta\tau^2\epsilon\varrho_{\{1,3\}}\varrho^2_{\{1,4\}}\varrho_{\{1,5\}}\varrho_{\{2,5\}}\varrho^3_{\{1,1\}}\\
&-6\eta\tau^2\epsilon\varrho_{\{1,2\}}\varrho^2_{\{1,4\}}\varrho_{\{1,5\}}\varrho_{\{2,3\}}\varrho_{\{2,5\}}\varrho^2_{\{1,1\}} - 8\eta\tau^2\epsilon\varrho_{\{1,2\}}\varrho_{\{1,3\}}\varrho_{\{1,4\}}\varrho_{\{1,5\}}\varrho_{\{2,4\}}\varrho_{\{2,5\}}\varrho^2_{\{1,1\}} + 6\tau^2\varrho^2_{\{1,4\}}\varrho^2_{\{2,1\}}\varrho_{\{2,5\}} = 0,\\
&-96\gamma c_0\tau^4\varrho^3_{\{1,1\}}\varrho_{\{1,2\}}\varrho_{\{1,4\}}\varrho_{\{2,4\}}\varrho_{\{2,5\}} - 28\tau^3\epsilon\vartheta_4\varrho^2_{\{1,1\}}\varrho_{\{1,2\}}\varrho^2_{\{1,4\}}\varrho_{\{2,4\}}\varrho^2_{\{2,5\}} - 6\tau^3\epsilon\varrho^2_{\{1,1\}}\varrho_{\{1,2\}}\varrho^2_{\{1,4\}}\varrho_{\{1,5\}}\varrho_{\{2,3\}}\varrho_{\{2,5\}}\\
&-8\tau^3\epsilon\varrho^2_{\{1,1\}}\varrho_{\{1,2\}}\varrho_{\{1,3\}}\varrho_{\{1,4\}}\varrho_{\{1,5\}}\varrho_{\{2,4\}}\varrho_{\{2,5\}} = 0,\\
&-240\gamma c_0\tau^4\varrho^2_{\{1,4\}}\varrho_{\{2,5\}}\varrho^4_{\{1,1\}} - 20\tau^3\epsilon\vartheta_4\varrho^3_{\{1,4\}}\varrho^2_{\{2,5\}}\varrho^3_{\{1,1\}} - 10\tau^3\epsilon\varrho_{\{1,3\}}\varrho^2_{\{1,4\}}\varrho_{\{1,5\}}\varrho_{\{2,5\}}\varrho^3_{\{1,1\}} = 0,\\
&-20\tau^3\epsilon\varrho^3_{\{1,1\}}\varrho^3_{\{1,4\}}\varrho_{\{2,4\}}\varrho^2_{\{2,5\}} = 0,\\
&-96\gamma c_0\tau^4\vartheta_4\varrho_{\{1,4\}}\varrho_{\{2,5\}}\varrho^4_{\{1,1\}} - 48\gamma c_0\tau^4\varrho_{\{1,3\}}\varrho_{\{1,5\}}\varrho^4_{\{1,1\}} - 28\eta\tau^2\epsilon\varrho^4_{\{1,4\}}\varrho^2_{\{2,5\}}\varrho^3_{\{1,1\}} - 20\eta\tau^2\epsilon\varrho_{\{1,2\}}\varrho^3_{\{1,4\}}\varrho_{\{2,4\}}\varrho^2_{\{2,5\}}\varrho^2_{\{1,1\}}\\
&-8\tau^3\epsilon\vartheta_4^2\varrho^2_{\{1,4\}}\varrho^2_{\{2,5\}}\varrho^3_{\{1,1\}} - 8\tau^3\epsilon\vartheta_4\varrho_{\{1,3\}}\varrho_{\{1,4\}}\varrho_{\{1,5\}}\varrho_{\{2,5\}}\varrho^3_{\{1,1\}} - 2\tau^3\epsilon\varrho^2_{\{1,3\}}\varrho^2_{\{1,5\}}\varrho^3_{\{1,1\}} = 0,\\
&-160\gamma c_0\eta\tau^3\varrho_{\{1,4\}}\varrho_{\{2,4\}}\varrho_{\{2,5\}}\varrho^4_{\{1,1\}} - 96\gamma c_0\eta\tau^3\varrho^2_{\{1,2\}}\varrho_{\{1,4\}}\varrho_{\{2,4\}}\varrho_{\{2,5\}}\varrho^2_{\{1,1\}}\\
&-4c_0^2\tau^2\varrho_{\{1,4\}}\varrho_{\{2,4\}}\varrho_{\{2,5\}}\varrho^2_{\{1,1\}} - 32\eta\tau^2\epsilon\vartheta_4\varrho^2_{\{1,4\}}\varrho_{\{2,4\}}\varrho^2_{\{2,5\}}\varrho^3_{\{1,1\}}\\
&-16\eta\tau^2\epsilon\vartheta_4\varrho_{\{1,2\}}\varrho_{\{1,4\}}\varrho^2_{\{2,4\}}\varrho^2_{\{2,5\}}\varrho^2_{\{1,1\}} - 16\eta\tau^2\epsilon\vartheta_4\varrho^2_{\{1,2\}}\varrho^2_{\{1,4\}}\varrho_{\{2,4\}}\varrho^2_{\{2,5\}}\varrho_{\{1,1\}}\\
&-16\eta\tau^2\epsilon\varrho_{\{1,3\}}\varrho_{\{1,4\}}\varrho_{\{1,5\}}\varrho_{\{2,4\}}\varrho_{\{2,5\}}\varrho^3_{\{1,1\}} - 4\eta\tau^2\epsilon\varrho_{\{1,2\}}\varrho_{\{1,3\}}\varrho_{\{1,5\}}\varrho^2_{\{2,4\}}\varrho_{\{2,5\}}\varrho^2_{\{1,1\}}\\
&-4\eta\tau^2\epsilon\varrho_{\{1,2\}}\varrho_{\{1,4\}}\varrho_{\{1,5\}}\varrho_{\{2,3\}}\varrho_{\{2,4\}}\varrho_{\{2,5\}}\varrho^2_{\{1,1\}} - 4\eta\tau^2\epsilon\varrho^2_{\{1,2\}}\varrho^2_{\{1,4\}}\varrho_{\{1,5\}}\varrho_{\{2,3\}}\varrho_{\{2,5\}}\varrho_{\{1,1\}}\\
&-4\eta\tau^2\epsilon\varrho^2_{\{1,2\}}\varrho_{\{1,3\}}\varrho_{\{1,4\}}\varrho_{\{1,5\}}\varrho_{\{2,4\}}\varrho_{\{2,5\}}\varrho_{\{1,1\}} + 4\tau^2\varrho_{\{1,4\}}\varrho^2_{\{2,1\}}\varrho_{\{2,4\}}\varrho_{\{2,5\}} = 0,\\
&-96\gamma c_0\tau^4\varrho^2_{\{1,1\}}\varrho^2_{\{1,2\}}\varrho_{\{1,4\}}\varrho_{\{2,4\}}\varrho_{\{2,5\}} - 16\tau^3\epsilon\vartheta_4\varrho^2_{\{1,1\}}\varrho_{\{1,2\}}\varrho_{\{1,4\}}\varrho^2_{\{2,4\}}\varrho^2_{\{2,5\}} - 16\tau^3\epsilon\vartheta_4\varrho_{\{1,1\}}\varrho^2_{\{1,2\}}\varrho^2_{\{1,4\}}\varrho_{\{2,4\}}\varrho^2_{\{2,5\}}\\
&-4\tau^3\epsilon\varrho^2_{\{1,1\}}\varrho_{\{1,2\}}\varrho_{\{1,3\}}\varrho_{\{1,5\}}\varrho^2_{\{2,4\}}\varrho_{\{2,5\}} - 4\tau^3\epsilon\varrho_{\{1,1\}}\varrho^2_{\{1,2\}}\varrho^2_{\{1,4\}}\varrho_{\{1,5\}}\varrho_{\{2,3\}}\varrho_{\{2,5\}}\\
&-4\tau^3\epsilon\varrho_{\{1,1\}}\varrho^2_{\{1,2\}}\varrho_{\{1,3\}}\varrho_{\{1,4\}}\varrho_{\{1,5\}}\varrho_{\{2,4\}}\varrho_{\{2,5\}} - 4\tau^3\epsilon\varrho^2_{\{1,1\}}\varrho_{\{1,2\}}\varrho_{\{1,4\}}\varrho_{\{1,5\}}\varrho_{\{2,3\}}\varrho_{\{2,4\}}\varrho_{\{2,5\}} = 0,\\
&-272\gamma c_0\eta^2\tau^2\varrho^2_{\{1,4\}}\varrho_{\{2,5\}}\varrho^4_{\{1,1\}} - 128\gamma c_0\eta^2\tau^2\varrho_{\{1,2\}}\varrho_{\{1,4\}}\varrho_{\{2,4\}}\varrho_{\{2,5\}}\varrho^3_{\{1,1\}}\\
&-32\gamma c_0\eta^2\tau^2\varrho^3_{\{1,2\}}\varrho_{\{1,4\}}\varrho_{\{2,4\}}\varrho_{\{2,5\}}\varrho_{\{1,1\}} - 8c_0^2\eta\tau\varrho^2_{\{1,4\}}\varrho_{\{2,5\}}\varrho^2_{\{1,1\}} - 4c_0^2\eta\tau\varrho_{\{1,2\}}\varrho_{\{1,4\}}\varrho_{\{2,4\}}\varrho_{\{2,5\}}\varrho_{\{1,1\}}\\
&+8\eta\tau\varrho^2_{\{1,4\}}\varrho^2_{\{2,1\}}\varrho_{\{2,5\}} + 4\eta\tau\varrho_{\{1,4\}}\varrho_{\{2,1\}}\varrho_{\{2,2\}}\varrho_{\{2,4\}}\varrho_{\{2,5\}} - 28\eta^2\tau\epsilon\vartheta_4\varrho^3_{\{1,4\}}\varrho^2_{\{2,5\}}\varrho^3_{\{1,1\}}\\
&-40\eta^2\tau\epsilon\vartheta_4\varrho_{\{1,2\}}\varrho^2_{\{1,4\}}\varrho_{\{2,4\}}\varrho^2_{\{2,5\}}\varrho^2_{\{1,1\}} - 12\eta^2\tau\epsilon\vartheta_4\varrho^2_{\{1,2\}}\varrho_{\{1,4\}}\varrho^2_{\{2,4\}}\varrho^2_{\{2,5\}}\varrho_{\{1,1\}} - 14\eta^2\tau\epsilon\varrho_{\{1,3\}}\varrho^2_{\{1,4\}}\varrho_{\{1,5\}}\varrho_{\{2,5\}}\varrho^3_{\{1,1\}}\\
&-8\eta^2\tau\epsilon\varrho_{\{1,2\}}\varrho^2_{\{1,4\}}\varrho_{\{1,5\}}\varrho_{\{2,3\}}\varrho_{\{2,5\}}\varrho^2_{\{1,1\}} - 12\eta^2\tau\epsilon\varrho_{\{1,2\}}\varrho_{\{1,3\}}\varrho_{\{1,4\}}\varrho_{\{1,5\}}\varrho_{\{2,4\}}\varrho_{\{2,5\}}\varrho^2_{\{1,1\}}\\
&-2\eta^2\tau\epsilon\varrho^2_{\{1,2\}}\varrho_{\{1,3\}}\varrho_{\{1,5\}}\varrho^2_{\{2,4\}}\varrho_{\{2,5\}}\varrho_{\{1,1\}} - 4\eta^2\tau\epsilon\varrho^2_{\{1,2\}}\varrho_{\{1,4\}}\varrho_{\{1,5\}}\varrho_{\{2,3\}}\varrho_{\{2,4\}}\varrho_{\{2,5\}}\varrho_{\{1,1\}} = 0,\\
&-128\gamma c_0\eta\tau^3\varrho_{\{1,2\}}\varrho_{\{1,4\}}\varrho_{\{2,4\}}\varrho_{\{2,5\}}\varrho^3_{\{1,1\}} - 128\gamma c_0\eta\tau^3\varrho^3_{\{1,2\}}\varrho_{\{1,4\}}\varrho_{\{2,4\}}\varrho_{\{2,5\}}\varrho_{\{1,1\}} - 4c_0^2\tau^2\varrho_{\{1,2\}}\varrho_{\{1,4\}}\varrho_{\{2,4\}}\varrho_{\{2,5\}}\varrho_{\{1,1\}}\\
&-40\eta\tau^2\epsilon\vartheta_4\varrho_{\{1,2\}}\varrho^2_{\{1,4\}}\varrho_{\{2,4\}}\varrho^2_{\{2,5\}}\varrho^2_{\{1,1\}} - 40\eta\tau^2\epsilon\vartheta_4\varrho^2_{\{1,2\}}\varrho_{\{1,4\}}\varrho^2_{\{2,4\}}\varrho^2_{\{2,5\}}\varrho_{\{1,1\}}\\
&-8\eta\tau^2\epsilon\varrho_{\{1,2\}}\varrho^2_{\{1,4\}}\varrho_{\{1,5\}}\varrho_{\{2,3\}}\varrho_{\{2,5\}}\varrho^2_{\{1,1\}} - 12\eta\tau^2\epsilon\varrho_{\{1,2\}}\varrho_{\{1,3\}}\varrho_{\{1,4\}}\varrho_{\{1,5\}}\varrho_{\{2,4\}}\varrho_{\{2,5\}}\varrho^2_{\{1,1\}}\\
&-8\eta\tau^2\epsilon\varrho^2_{\{1,2\}}\varrho_{\{1,3\}}\varrho_{\{1,5\}}\varrho^2_{\{2,4\}}\varrho_{\{2,5\}}\varrho_{\{1,1\}} - 12\eta\tau^2\epsilon\varrho^2_{\{1,2\}}\varrho_{\{1,4\}}\varrho_{\{1,5\}}\varrho_{\{2,3\}}\varrho_{\{2,4\}}\varrho_{\{2,5\}}\varrho_{\{1,1\}}\\
&+4\tau^2\varrho_{\{1,4\}}\varrho_{\{2,1\}}\varrho_{\{2,2\}}\varrho_{\{2,4\}}\varrho_{\{2,5\}} = 0,
\end{aligned}
$$

$$
\begin{aligned}
&-96\gamma c_0\tau^4\varrho_{\{1,1\}}\varrho_{\{1,2\}}^3\varrho_{\{1,4\}}\varrho_{\{2,4\}}\varrho_{\{2,5\}} - 28\tau^3\epsilon\vartheta_4\varrho_{\{1,1\}}\varrho_{\{1,2\}}^2\varrho_{\{1,4\}}\varrho_{\{2,4\}}^2\varrho_{\{2,5\}}^2 - 6\tau^3\epsilon\varrho_{\{1,1\}}\varrho_{\{1,2\}}^2\varrho_{\{1,3\}}\varrho_{\{1,5\}}\varrho_{\{2,4\}}^2\varrho_{\{2,5\}} \\
&-8\tau^3\epsilon\varrho_{\{1,1\}}\varrho_{\{1,2\}}^2\varrho_{\{1,4\}}\varrho_{\{1,5\}}\varrho_{\{2,3\}}\varrho_{\{2,4\}}\varrho_{\{2,5\}} = 0, \\
&-64\gamma c_0\eta^2\tau^2\varrho_{\{1,4\}}\varrho_{\{2,4\}}\varrho_{\{2,5\}}\varrho_{\{1,1\}}^4 - 96\gamma c_0\eta^2\tau^2\varrho_{\{1,2\}}^2\varrho_{\{1,4\}}\varrho_{\{2,4\}}\varrho_{\{2,5\}}\varrho_{\{1,1\}}^2 \\
&-64\gamma c_0\eta^2\tau^2\varrho_{\{1,2\}}^4\varrho_{\{1,4\}}\varrho_{\{2,4\}}\varrho_{\{2,5\}} - 4c_0^2\eta\tau\varrho_{\{1,4\}}\varrho_{\{2,4\}}\varrho_{\{2,5\}}\varrho_{\{1,1\}}^2 - 4c_0^2\eta\tau\varrho_{\{1,2\}}^2\varrho_{\{1,4\}}\varrho_{\{2,4\}}\varrho_{\{2,5\}} \\
&+4\eta\tau\varrho_{\{1,4\}}\varrho_{\{2,1\}}^2\varrho_{\{2,4\}}\varrho_{\{2,5\}} + 4\eta\tau\varrho_{\{1,4\}}\varrho_{\{2,2\}}^2\varrho_{\{2,4\}}\varrho_{\{2,5\}} - 16\eta^2\tau\epsilon\vartheta_4\varrho_{\{1,4\}}^2\varrho_{\{2,4\}}\varrho_{\{2,5\}}^2\varrho_{\{1,1\}}^3 \\
&-16\eta^2\tau\epsilon\vartheta_4\varrho_{\{1,2\}}\varrho_{\{1,4\}}\varrho_{\{2,4\}}^2\varrho_{\{2,5\}}^2\varrho_{\{1,1\}}^2 - 16\eta^2\tau\epsilon\vartheta_4\varrho_{\{1,2\}}^2\varrho_{\{1,4\}}^2\varrho_{\{2,4\}}\varrho_{\{2,5\}}^2\varrho_{\{1,1\}} \\
&-16\eta^2\tau\epsilon\vartheta_4\varrho_{\{1,2\}}^3\varrho_{\{1,4\}}\varrho_{\{2,4\}}^2\varrho_{\{2,5\}}^2 - 8\eta^2\tau\epsilon\varrho_{\{1,3\}}\varrho_{\{1,4\}}\varrho_{\{1,5\}}\varrho_{\{2,4\}}\varrho_{\{2,5\}}\varrho_{\{1,1\}}^3 - 4\eta^2\tau\epsilon\varrho_{\{1,2\}}\varrho_{\{1,3\}}\varrho_{\{1,5\}}\varrho_{\{2,4\}}^2\varrho_{\{2,5\}}\varrho_{\{1,1\}}^2 \\
&-4\eta^2\tau\epsilon\varrho_{\{1,2\}}\varrho_{\{1,4\}}\varrho_{\{1,5\}}\varrho_{\{2,3\}}\varrho_{\{2,4\}}\varrho_{\{2,5\}}\varrho_{\{1,1\}}^2 - 4\eta^2\tau\epsilon\varrho_{\{1,2\}}^2\varrho_{\{1,4\}}^2\varrho_{\{1,5\}}\varrho_{\{2,3\}}\varrho_{\{2,5\}}\varrho_{\{1,1\}} \\
&-4\eta^2\tau\epsilon\varrho_{\{1,2\}}^2\varrho_{\{1,3\}}\varrho_{\{1,4\}}\varrho_{\{1,5\}}\varrho_{\{2,4\}}\varrho_{\{2,5\}}\varrho_{\{1,1\}} - 8\eta^2\tau\epsilon\varrho_{\{1,2\}}^3\varrho_{\{1,4\}}\varrho_{\{1,5\}}\varrho_{\{2,3\}}\varrho_{\{2,4\}}\varrho_{\{2,5\}} = 0, \\
&-160\gamma c_0\eta\tau^3\varrho_{\{1,4\}}\varrho_{\{2,4\}}\varrho_{\{2,5\}}\varrho_{\{1,2\}}^4 - 96\gamma c_0\eta\tau^3\varrho_{\{1,1\}}^2\varrho_{\{1,4\}}\varrho_{\{2,4\}}\varrho_{\{2,5\}}\varrho_{\{1,2\}}^2 \\
&-4c_0^2\tau^2\varrho_{\{1,4\}}\varrho_{\{2,4\}}\varrho_{\{2,5\}}\varrho_{\{1,2\}}^2 - 32\eta\tau^2\epsilon\vartheta_4\varrho_{\{1,4\}}\varrho_{\{2,4\}}^2\varrho_{\{2,5\}}^2\varrho_{\{1,2\}}^3 \\
&-16\eta\tau^2\epsilon\vartheta_4\varrho_{\{1,1\}}\varrho_{\{1,4\}}^2\varrho_{\{2,4\}}\varrho_{\{2,5\}}^2\varrho_{\{1,2\}}^2 - 16\eta\tau^2\epsilon\vartheta_4\varrho_{\{1,1\}}^2\varrho_{\{1,4\}}\varrho_{\{2,4\}}^2\varrho_{\{2,5\}}^2\varrho_{\{1,2\}} \\
&-16\eta\tau^2\epsilon\varrho_{\{1,4\}}\varrho_{\{1,5\}}\varrho_{\{2,3\}}\varrho_{\{2,4\}}\varrho_{\{2,5\}}\varrho_{\{1,2\}}^3 - 4\eta\tau^2\epsilon\varrho_{\{1,1\}}\varrho_{\{1,4\}}^2\varrho_{\{1,5\}}\varrho_{\{2,3\}}\varrho_{\{2,5\}}\varrho_{\{1,2\}}^2 \\
&-4\eta\tau^2\epsilon\varrho_{\{1,1\}}\varrho_{\{1,3\}}\varrho_{\{1,4\}}\varrho_{\{1,5\}}\varrho_{\{2,4\}}\varrho_{\{2,5\}}\varrho_{\{1,2\}}^2 - 4\eta\tau^2\epsilon\varrho_{\{1,1\}}^2\varrho_{\{1,3\}}\varrho_{\{1,5\}}\varrho_{\{2,4\}}^2\varrho_{\{2,5\}}\varrho_{\{1,2\}} \\
&-4\eta\tau^2\epsilon\varrho_{\{1,1\}}^2\varrho_{\{1,4\}}\varrho_{\{1,5\}}\varrho_{\{2,3\}}\varrho_{\{2,4\}}\varrho_{\{2,5\}}\varrho_{\{1,2\}} + 4\tau^2\varrho_{\{1,4\}}\varrho_{\{2,2\}}^2\varrho_{\{2,4\}}\varrho_{\{2,5\}} = 0, \\
&-96\gamma c_0\tau^4\varrho_{\{1,4\}}\varrho_{\{2,4\}}\varrho_{\{2,5\}}\varrho_{\{1,2\}}^4 - 16\tau^3\epsilon\vartheta_4\varrho_{\{1,4\}}\varrho_{\{2,4\}}^2\varrho_{\{2,5\}}^2\varrho_{\{1,2\}}^3 - 8\tau^3\epsilon\varrho_{\{1,4\}}\varrho_{\{1,5\}}\varrho_{\{2,3\}}\varrho_{\{2,4\}}\varrho_{\{2,5\}}\varrho_{\{1,2\}}^3 = 0, \\
&-8\tau^3\epsilon\varrho_{\{1,4\}}^2\varrho_{\{2,4\}}^2\varrho_{\{2,5\}}^2\varrho_{\{1,1\}}^3 - 20\tau^3\epsilon\varrho_{\{1,2\}}\varrho_{\{1,4\}}^3\varrho_{\{2,4\}}\varrho_{\{2,5\}}^2\varrho_{\{1,1\}}^2 = 0, \\
&-44\eta\tau^2\epsilon\varrho_{\{1,1\}}^3\varrho_{\{2,4\}}\varrho_{\{2,5\}}^2\varrho_{\{1,4\}}^3 - 8\eta\tau^2\epsilon\varrho_{\{1,1\}}\varrho_{\{1,2\}}^2\varrho_{\{2,4\}}\varrho_{\{2,5\}}^2\varrho_{\{1,4\}}^3 - 28\eta\tau^2\epsilon\varrho_{\{1,1\}}^2\varrho_{\{1,2\}}\varrho_{\{2,4\}}^2\varrho_{\{2,5\}}^2\varrho_{\{1,4\}}^2 = 0, \\
&-28\tau^3\epsilon\varrho_{\{1,1\}}^2\varrho_{\{1,2\}}\varrho_{\{1,4\}}^2\varrho_{\{2,4\}}^2\varrho_{\{2,5\}}^2 - 8\tau^3\epsilon\varrho_{\{1,1\}}\varrho_{\{1,2\}}^2\varrho_{\{1,4\}}^3\varrho_{\{2,4\}}\varrho_{\{2,5\}}^2 = 0, \\
&-160\gamma c_0\eta\tau^3\vartheta_4\varrho_{\{1,4\}}\varrho_{\{2,5\}}\varrho_{\{1,1\}}^4 - 80\gamma c_0\eta\tau^3\varrho_{\{1,3\}}\varrho_{\{1,5\}}\varrho_{\{1,1\}}^4 - 4c_0^2\tau^2\vartheta_4\varrho_{\{1,4\}}\varrho_{\{2,5\}}\varrho_{\{1,1\}}^2 \\
&-2c_0^2\tau^2\varrho_{\{1,3\}}\varrho_{\{1,5\}}\varrho_{\{1,1\}}^2 - 20\eta^2\tau\epsilon\varrho_{\{1,4\}}^4\varrho_{\{2,5\}}^2\varrho_{\{1,1\}}^3 - 32\eta^2\tau\epsilon\varrho_{\{1,2\}}\varrho_{\{1,4\}}^3\varrho_{\{2,4\}}\varrho_{\{2,5\}}^2\varrho_{\{1,1\}}^2 \\
&-12\eta^2\tau\epsilon\varrho_{\{1,2\}}^2\varrho_{\{1,4\}}^2\varrho_{\{2,4\}}^2\varrho_{\{2,5\}}^2\varrho_{\{1,1\}} - 16\eta\tau^2\epsilon\vartheta_4^2\varrho_{\{1,4\}}^2\varrho_{\{2,5\}}^2\varrho_{\{1,1\}}^3 - 16\eta\tau^2\epsilon\vartheta_4\varrho_{\{1,3\}}\varrho_{\{1,4\}}\varrho_{\{1,5\}}\varrho_{\{2,5\}}\varrho_{\{1,1\}}^3 \\
&-8\eta\tau^2\epsilon\vartheta_4^2\varrho_{\{1,2\}}\varrho_{\{1,4\}}\varrho_{\{2,4\}}\varrho_{\{2,5\}}^2\varrho_{\{1,1\}}^2 - 4\eta\tau^2\epsilon\vartheta_4\varrho_{\{1,2\}}\varrho_{\{1,4\}}\varrho_{\{1,5\}}\varrho_{\{2,3\}}\varrho_{\{2,5\}}\varrho_{\{1,1\}}^2 \\
&-4\eta\tau^2\epsilon\vartheta_4\varrho_{\{1,2\}}\varrho_{\{1,3\}}\varrho_{\{1,5\}}\varrho_{\{2,4\}}\varrho_{\{2,5\}}\varrho_{\{1,1\}}^2 - 4\eta\tau^2\epsilon\varrho_{\{1,3\}}^2\varrho_{\{1,5\}}^2\varrho_{\{1,1\}}^3 \\
&-2\eta\tau^2\epsilon\varrho_{\{1,2\}}\varrho_{\{1,3\}}\varrho_{\{1,5\}}^2\varrho_{\{2,3\}}\varrho_{\{1,1\}}^2 + 4\tau^2\vartheta_4\varrho_{\{1,4\}}\varrho_{\{2,1\}}^2\varrho_{\{2,5\}} + 2\tau^2\varrho_{\{1,3\}}\varrho_{\{1,5\}}\varrho_{\{2,1\}}^2 = 0, \\
&-272\gamma c_0\eta^2\tau^2\varrho_{\{2,4\}}^2\varrho_{\{2,5\}}\varrho_{\{1,2\}}^4 - 128\gamma c_0\eta^2\tau^2\varrho_{\{1,1\}}\varrho_{\{1,4\}}\varrho_{\{2,4\}}\varrho_{\{2,5\}}\varrho_{\{1,2\}}^3 \\
&-32\gamma c_0\eta^2\tau^2\varrho_{\{1,1\}}^3\varrho_{\{1,4\}}\varrho_{\{2,4\}}\varrho_{\{2,5\}}\varrho_{\{1,2\}} - 8c_0^2\eta\tau\varrho_{\{2,4\}}^2\varrho_{\{2,5\}}\varrho_{\{1,2\}}^2 \\
&-4c_0^2\eta\tau\varrho_{\{1,1\}}\varrho_{\{1,4\}}\varrho_{\{2,4\}}\varrho_{\{2,5\}}\varrho_{\{1,2\}} + 8\eta\tau\varrho_{\{2,2\}}^2\varrho_{\{2,4\}}^2\varrho_{\{2,5\}} \\
&+4\eta\tau\varrho_{\{1,4\}}\varrho_{\{2,1\}}\varrho_{\{2,2\}}\varrho_{\{2,4\}}\varrho_{\{2,5\}} \\
&-28\eta^2\tau\epsilon\vartheta_4\varrho_{\{2,4\}}^3\varrho_{\{2,5\}}^2\varrho_{\{1,2\}}^3 - 40\eta^2\tau\epsilon\vartheta_4\varrho_{\{1,1\}}\varrho_{\{1,4\}}\varrho_{\{2,4\}}^2\varrho_{\{2,5\}}^2\varrho_{\{1,2\}}^2 \\
&-12\eta^2\tau\epsilon\vartheta_4\varrho_{\{1,1\}}^2\varrho_{\{1,4\}}^2\varrho_{\{2,4\}}\varrho_{\{2,5\}}^2\varrho_{\{1,2\}} - 14\eta^2\tau\epsilon\varrho_{\{1,5\}}\varrho_{\{2,3\}}\varrho_{\{2,4\}}^2\varrho_{\{2,5\}}\varrho_{\{1,2\}}^3 \\
&-8\eta^2\tau\epsilon\varrho_{\{1,1\}}\varrho_{\{1,3\}}\varrho_{\{1,5\}}\varrho_{\{2,4\}}^2\varrho_{\{2,5\}}\varrho_{\{1,2\}}^2 - 12\eta^2\tau\epsilon\varrho_{\{1,1\}}\varrho_{\{1,4\}}\varrho_{\{1,5\}}\varrho_{\{2,3\}}\varrho_{\{2,4\}}\varrho_{\{2,5\}}\varrho_{\{1,2\}}^2 \\
&-2\eta^2\tau\epsilon\varrho_{\{1,1\}}^2\varrho_{\{1,4\}}^2\varrho_{\{1,5\}}\varrho_{\{2,3\}}\varrho_{\{2,5\}}\varrho_{\{1,2\}} - 4\eta^2\tau\epsilon\varrho_{\{1,1\}}^2\varrho_{\{1,3\}}\varrho_{\{1,4\}}\varrho_{\{1,5\}}\varrho_{\{2,4\}}\varrho_{\{2,5\}}\varrho_{\{1,2\}} = 0, \\
&-480\gamma c_0\eta\tau^3\varrho_{\{2,4\}}^2\varrho_{\{2,5\}}\varrho_{\{1,2\}}^4 - 96\gamma c_0\eta\tau^3\varrho_{\{1,1\}}\varrho_{\{1,4\}}\varrho_{\{2,4\}}\varrho_{\{2,5\}}\varrho_{\{1,2\}}^3 \\
&-6c_0^2\tau^2\varrho_{\{2,4\}}^2\varrho_{\{2,5\}}\varrho_{\{1,2\}}^2 - 44\eta\tau^2\epsilon\vartheta_4\varrho_{\{2,4\}}^3\varrho_{\{2,5\}}^2\varrho_{\{1,2\}}^3 - 28\eta\tau^2\epsilon\vartheta_4\varrho_{\{1,1\}}\varrho_{\{1,4\}}\varrho_{\{2,4\}}^2\varrho_{\{2,5\}}^2\varrho_{\{1,2\}}^2 \\
&-22\eta\tau^2\epsilon\varrho_{\{1,5\}}\varrho_{\{2,3\}}\varrho_{\{2,4\}}^2\varrho_{\{2,5\}}\varrho_{\{1,2\}}^3 - 6\eta\tau^2\epsilon\varrho_{\{1,1\}}\varrho_{\{1,3\}}\varrho_{\{1,5\}}\varrho_{\{2,4\}}^2\varrho_{\{2,5\}}\varrho_{\{1,2\}}^2
\end{aligned}
$$

$$\begin{aligned}
-8\eta\tau^2\epsilon\varrho_{\{1,1\}}\varrho_{\{1,4\}}\varrho_{\{1,5\}}\varrho_{\{2,3\}}\varrho_{\{2,4\}}\varrho_{\{2,5\}}\varrho_{\{1,2\}}^2 + 6\tau^2\varrho_{\{2,2\}}^2\varrho_{\{2,4\}}^2\varrho_{\{2,5\}} &= 0,\\
-240\gamma c_0\tau^4\varrho_{\{2,4\}}^2\varrho_{\{2,5\}}\varrho_{\{1,2\}}^4 - 20\tau^3\epsilon\vartheta_4\varrho_{\{2,4\}}^3\varrho_{\{2,5\}}^2\varrho_{\{1,2\}}^3 - 10\tau^3\epsilon\varrho_{\{1,5\}}\varrho_{\{2,3\}}\varrho_{\{2,4\}}^2\varrho_{\{2,5\}}\varrho_{\{1,2\}}^3 &= 0,\\
-8\eta\tau^2\epsilon\varrho_{\{1,1\}}^2\varrho_{\{1,2\}}\varrho_{\{1,4\}}\varrho_{\{2,4\}}^3\varrho_{\{2,5\}}^2 - 16\eta\tau^2\epsilon\varrho_{\{1,1\}}^3\varrho_{\{1,4\}}^2\varrho_{\{2,4\}}^2\varrho_{\{2,5\}}^2 &\\
-40\eta\tau^2\epsilon\varrho_{\{1,1\}}\varrho_{\{1,2\}}^2\varrho_{\{1,4\}}^2\varrho_{\{2,4\}}^2\varrho_{\{2,5\}}^2 - 32\eta\tau^2\epsilon\varrho_{\{1,1\}}^2\varrho_{\{1,2\}}\varrho_{\{1,4\}}^3\varrho_{\{2,4\}}\varrho_{\{2,5\}}^2 &\\
-8\tau^3\epsilon\vartheta_4^2\varrho_{\{1,1\}}^2\varrho_{\{1,2\}}\varrho_{\{1,4\}}\varrho_{\{2,4\}}\varrho_{\{2,5\}}^2 - 4\tau^3\epsilon\vartheta_4\varrho_{\{1,1\}}^2\varrho_{\{1,2\}}\varrho_{\{1,4\}}\varrho_{\{1,5\}}\varrho_{\{2,3\}}\varrho_{\{2,5\}} &\\
-4\tau^3\epsilon\vartheta_4\varrho_{\{1,1\}}^2\varrho_{\{1,2\}}\varrho_{\{1,3\}}\varrho_{\{1,5\}}\varrho_{\{2,4\}}\varrho_{\{2,5\}} - 2\tau^3\epsilon\varrho_{\{1,1\}}^2\varrho_{\{1,2\}}\varrho_{\{1,3\}}\varrho_{\{1,5\}}^2\varrho_{\{2,3\}} &= 0,\\
-8\tau^3\epsilon\varrho_{\{1,1\}}^2\varrho_{\{1,2\}}\varrho_{\{1,4\}}\varrho_{\{2,4\}}^3\varrho_{\{2,5\}}^2 - 28\tau^3\epsilon\varrho_{\{1,1\}}\varrho_{\{1,2\}}^2\varrho_{\{1,4\}}^2\varrho_{\{2,4\}}^2\varrho_{\{2,5\}}^2 &= 0,\\
-8\eta^2\tau\epsilon\varrho_{\{1,4\}}^2\varrho_{\{2,4\}}^2\varrho_{\{2,5\}}^2\varrho_{\{1,2\}}^3 - 12\eta^2\tau\epsilon\varrho_{\{1,1\}}\varrho_{\{1,4\}}\varrho_{\{2,4\}}^3\varrho_{\{2,5\}}^2\varrho_{\{1,2\}}^2 &\\
-8\eta^2\tau\epsilon\varrho_{\{1,1\}}\varrho_{\{1,4\}}^3\varrho_{\{2,4\}}\varrho_{\{2,5\}}^2\varrho_{\{1,2\}}^2 - 40\eta^2\tau\epsilon\varrho_{\{1,1\}}^2\varrho_{\{1,4\}}^2\varrho_{\{2,4\}}^2\varrho_{\{2,5\}}^2\varrho_{\{1,2\}} &\\
-28\eta^2\tau\epsilon\varrho_{\{1,1\}}^3\varrho_{\{1,4\}}^3\varrho_{\{2,4\}}\varrho_{\{2,5\}}^2 - 8\eta\tau^2\epsilon\vartheta_4^2\varrho_{\{1,1\}}\varrho_{\{1,4\}}\varrho_{\{2,4\}}\varrho_{\{2,5\}}^2\varrho_{\{1,2\}}^2 &\\
-4\eta\tau^2\epsilon\vartheta_4\varrho_{\{1,1\}}\varrho_{\{1,4\}}\varrho_{\{1,5\}}\varrho_{\{2,3\}}\varrho_{\{2,5\}}\varrho_{\{1,2\}}^2 - 4\eta\tau^2\epsilon\vartheta_4\varrho_{\{1,1\}}\varrho_{\{1,3\}}\varrho_{\{1,5\}}\varrho_{\{2,4\}}\varrho_{\{2,5\}}\varrho_{\{1,2\}}^2 &\\
-2\eta\tau^2\epsilon\varrho_{\{1,1\}}\varrho_{\{1,3\}}\varrho_{\{1,5\}}^2\varrho_{\{2,3\}}\varrho_{\{1,2\}}^2 &= 0,\\
-32\eta\tau^2\epsilon\varrho_{\{1,1\}}\varrho_{\{1,2\}}^2\varrho_{\{1,4\}}\varrho_{\{2,4\}}^3\varrho_{\{2,5\}}^2 - 16\eta\tau^2\epsilon\varrho_{\{1,2\}}^3\varrho_{\{1,4\}}^2\varrho_{\{2,4\}}^2\varrho_{\{2,5\}}^2 &\\
-40\eta\tau^2\epsilon\varrho_{\{1,1\}}^2\varrho_{\{1,2\}}\varrho_{\{1,4\}}^2\varrho_{\{2,4\}}^2\varrho_{\{2,5\}}^2 - 8\eta\tau^2\epsilon\varrho_{\{1,1\}}\varrho_{\{1,2\}}^2\varrho_{\{1,4\}}^3\varrho_{\{2,4\}}\varrho_{\{2,5\}}^2 &\\
-8\tau^3\epsilon\vartheta_4^2\varrho_{\{1,1\}}\varrho_{\{1,2\}}^2\varrho_{\{1,4\}}\varrho_{\{2,4\}}\varrho_{\{2,5\}}^2 - 4\tau^3\epsilon\vartheta_4\varrho_{\{1,1\}}\varrho_{\{1,2\}}^2\varrho_{\{1,4\}}\varrho_{\{1,5\}}\varrho_{\{2,3\}}\varrho_{\{2,5\}} &\\
-4\tau^3\epsilon\vartheta_4\varrho_{\{1,1\}}\varrho_{\{1,2\}}^2\varrho_{\{1,3\}}\varrho_{\{1,5\}}\varrho_{\{2,4\}}\varrho_{\{2,5\}} - 2\tau^3\epsilon\varrho_{\{1,1\}}\varrho_{\{1,2\}}^2\varrho_{\{1,3\}}\varrho_{\{1,5\}}^2\varrho_{\{2,3\}} &= 0,\\
-8\tau^3\epsilon\varrho_{\{1,4\}}^2\varrho_{\{2,4\}}^2\varrho_{\{2,5\}}^2\varrho_{\{1,2\}}^3 - 20\tau^3\epsilon\varrho_{\{1,1\}}\varrho_{\{1,4\}}\varrho_{\{2,4\}}^3\varrho_{\{2,5\}}^2\varrho_{\{1,2\}}^2 &= 0,\\
-64\gamma c_0\eta^2\tau^2\vartheta_4\varrho_{\{1,4\}}\varrho_{\{2,5\}}\varrho_{\{1,1\}}^4 - 32\gamma c_0\eta^2\tau^2\varrho_{\{1,3\}}\varrho_{\{1,5\}}\varrho_{\{1,1\}}^4 &\\
-4c_0^2\eta\tau\vartheta_4\varrho_{\{1,4\}}\varrho_{\{2,5\}}\varrho_{\{1,1\}}^2 - 2c_0^2\eta\tau\varrho_{\{1,3\}}\varrho_{\{1,5\}}\varrho_{\{1,1\}}^2 &\\
+4\eta\tau\vartheta_4\varrho_{\{1,4\}}\varrho_{\{2,1\}}^2\varrho_{\{2,5\}} + 2\eta\tau\varrho_{\{1,3\}}\varrho_{\{1,5\}}\varrho_{\{2,1\}}^2 - 4\eta^3\epsilon\varrho_{\{1,4\}}^4\varrho_{\{2,5\}}^2\varrho_{\{1,1\}}^3 &\\
-12\eta^3\epsilon\varrho_{\{1,2\}}\varrho_{\{1,4\}}^3\varrho_{\{2,4\}}\varrho_{\{2,5\}}^2\varrho_{\{1,1\}}^2 - 12\eta^3\epsilon\varrho_{\{1,2\}}^2\varrho_{\{1,4\}}^2\varrho_{\{2,4\}}^2\varrho_{\{2,5\}}^2\varrho_{\{1,1\}} &\\
-4\eta^3\epsilon\varrho_{\{1,2\}}^3\varrho_{\{1,4\}}\varrho_{\{2,4\}}^3\varrho_{\{2,5\}}^2 - 8\eta^2\tau\epsilon\vartheta_4^2\varrho_{\{1,4\}}^2\varrho_{\{2,5\}}^2\varrho_{\{1,1\}}^3 &\\
-8\eta^2\tau\epsilon\vartheta_4\varrho_{\{1,3\}}\varrho_{\{1,4\}}\varrho_{\{1,5\}}\varrho_{\{2,5\}}\varrho_{\{1,1\}}^3 - 8\eta^2\tau\epsilon\vartheta_4^2\varrho_{\{1,2\}}\varrho_{\{1,4\}}\varrho_{\{2,4\}}\varrho_{\{2,5\}}^2\varrho_{\{1,1\}}^2 &\\
-4\eta^2\tau\epsilon\vartheta_4\varrho_{\{1,2\}}\varrho_{\{1,4\}}\varrho_{\{1,5\}}\varrho_{\{2,3\}}\varrho_{\{2,5\}}\varrho_{\{1,1\}}^2 - 4\eta^2\tau\epsilon\vartheta_4\varrho_{\{1,2\}}\varrho_{\{1,3\}}\varrho_{\{1,5\}}\varrho_{\{2,4\}}\varrho_{\{2,5\}}\varrho_{\{1,1\}}^2 &\\
-2\eta^2\tau\epsilon\varrho_{\{1,3\}}^2\varrho_{\{1,5\}}^2\varrho_{\{1,1\}}^3 - 2\eta^2\tau\epsilon\varrho_{\{1,2\}}\varrho_{\{1,3\}}\varrho_{\{1,5\}}^2\varrho_{\{2,3\}}\varrho_{\{1,1\}}^2 &= 0,\\
-8\eta^2\tau\epsilon\varrho_{\{1,4\}}^2\varrho_{\{2,4\}}^2\varrho_{\{2,5\}}^2\varrho_{\{1,1\}}^3 - 8\eta^2\tau\epsilon\varrho_{\{1,2\}}\varrho_{\{1,4\}}\varrho_{\{2,4\}}^3\varrho_{\{2,5\}}^2\varrho_{\{1,1\}}^2 &\\
-12\eta^2\tau\epsilon\varrho_{\{1,2\}}\varrho_{\{1,4\}}^3\varrho_{\{2,4\}}\varrho_{\{2,5\}}^2\varrho_{\{1,1\}}^2 - 40\eta^2\tau\epsilon\varrho_{\{1,2\}}^2\varrho_{\{1,4\}}^2\varrho_{\{2,4\}}^2\varrho_{\{2,5\}}^2\varrho_{\{1,1\}} &\\
-28\eta^2\tau\epsilon\varrho_{\{1,2\}}^3\varrho_{\{1,4\}}\varrho_{\{2,4\}}^3\varrho_{\{2,5\}}^2 - 8\eta\tau^2\epsilon\vartheta_4^2\varrho_{\{1,2\}}\varrho_{\{1,4\}}\varrho_{\{2,4\}}\varrho_{\{2,5\}}^2\varrho_{\{1,1\}}^2 &\\
-4\eta\tau^2\epsilon\vartheta_4\varrho_{\{1,2\}}\varrho_{\{1,4\}}\varrho_{\{1,5\}}\varrho_{\{2,3\}}\varrho_{\{2,5\}}\varrho_{\{1,1\}}^2 - 4\eta\tau^2\epsilon\vartheta_4\varrho_{\{1,2\}}\varrho_{\{1,3\}}\varrho_{\{1,5\}}\varrho_{\{2,4\}}\varrho_{\{2,5\}}\varrho_{\{1,1\}}^2 &\\
-2\eta\tau^2\epsilon\varrho_{\{1,2\}}\varrho_{\{1,3\}}\varrho_{\{1,5\}}^2\varrho_{\{2,3\}}\varrho_{\{1,1\}}^2 &= 0,\\
-44\eta\tau^2\epsilon\varrho_{\{1,2\}}^3\varrho_{\{1,4\}}\varrho_{\{2,5\}}^2\varrho_{\{2,4\}}^3 - 8\eta\tau^2\epsilon\varrho_{\{1,1\}}^2\varrho_{\{1,2\}}\varrho_{\{1,4\}}\varrho_{\{2,5\}}^2\varrho_{\{2,4\}}^3 - 28\eta\tau^2\epsilon\varrho_{\{1,1\}}\varrho_{\{1,2\}}^2\varrho_{\{1,4\}}^2\varrho_{\{2,5\}}^2\varrho_{\{2,4\}}^2 &= 0,\\
-64\gamma c_0\eta^2\tau^2\vartheta_4\varrho_{\{2,4\}}\varrho_{\{2,5\}}\varrho_{\{1,2\}}^4 - 32\gamma c_0\eta^2\tau^2\varrho_{\{1,5\}}\varrho_{\{2,3\}}\varrho_{\{1,2\}}^4 &\\
-4c_0^2\eta\tau\vartheta_4\varrho_{\{2,4\}}\varrho_{\{2,5\}}\varrho_{\{1,2\}}^2 - 2c_0^2\eta\tau\varrho_{\{1,5\}}\varrho_{\{2,3\}}\varrho_{\{1,2\}}^2 &\\
+4\eta\tau\vartheta_4\varrho_{\{2,2\}}^2\varrho_{\{2,4\}}\varrho_{\{2,5\}} + 2\eta\tau\varrho_{\{1,5\}}\varrho_{\{2,2\}}^2\varrho_{\{2,3\}} - 4\eta^3\epsilon\varrho_{\{2,4\}}^4\varrho_{\{2,5\}}^2\varrho_{\{1,2\}}^3 &\\
-12\eta^3\epsilon\varrho_{\{1,1\}}\varrho_{\{1,4\}}\varrho_{\{2,4\}}^3\varrho_{\{2,5\}}^2\varrho_{\{1,2\}}^2 - 12\eta^3\epsilon\varrho_{\{1,1\}}^2\varrho_{\{1,4\}}^2\varrho_{\{2,4\}}^2\varrho_{\{2,5\}}^2\varrho_{\{1,2\}} &\\
-4\eta^3\epsilon\varrho_{\{1,1\}}^3\varrho_{\{1,4\}}^3\varrho_{\{2,4\}}\varrho_{\{2,5\}}^2 - 8\eta^2\tau\epsilon\vartheta_4^2\varrho_{\{2,4\}}^2\varrho_{\{2,5\}}^2\varrho_{\{1,2\}}^3 &
\end{aligned}$$

$$
\begin{aligned}
&-8\eta^2\tau\epsilon\vartheta_4\varrho_{\{1,5\}}\varrho_{\{2,3\}}\varrho_{\{2,4\}}\varrho_{\{2,5\}}\varrho_{\{1,2\}}^3-8\eta^2\tau\epsilon\vartheta_4^2\varrho_{\{1,1\}}\varrho_{\{1,4\}}\varrho_{\{2,4\}}\varrho_{\{2,5\}}^2\varrho_{\{1,2\}}^2\\
&-4\eta^2\tau\epsilon\vartheta_4\varrho_{\{1,1\}}\varrho_{\{1,4\}}\varrho_{\{1,5\}}\varrho_{\{2,3\}}\varrho_{\{2,5\}}\varrho_{\{1,2\}}^2-4\eta^2\tau\epsilon\vartheta_4\varrho_{\{1,1\}}\varrho_{\{1,3\}}\varrho_{\{1,5\}}\varrho_{\{2,4\}}\varrho_{\{2,5\}}\varrho_{\{1,2\}}^2\\
&-2\eta^2\tau\epsilon\varrho_{\{1,5\}}^2\varrho_{\{2,3\}}^2\varrho_{\{1,2\}}^3-2\eta^2\tau\epsilon\varrho_{\{1,1\}}\varrho_{\{1,3\}}\varrho_{\{1,5\}}^2\varrho_{\{2,3\}}\varrho_{\{1,2\}}^2=0,\\
&-160\gamma c_0\eta\tau^3\vartheta_4\varrho_{\{2,4\}}\varrho_{\{2,5\}}\varrho_{\{1,2\}}^4-80\gamma c_0\eta\tau^3\varrho_{\{1,5\}}\varrho_{\{2,3\}}\varrho_{\{1,2\}}^4\\
&-4c_0^2\tau^2\vartheta_4\varrho_{\{2,4\}}\varrho_{\{2,5\}}\varrho_{\{1,2\}}^2-2c_0^2\tau^2\varrho_{\{1,5\}}\varrho_{\{2,3\}}\varrho_{\{1,2\}}^2\\
&-20\eta^2\tau\epsilon\varrho_{\{2,4\}}^4\varrho_{\{2,5\}}^2\varrho_{\{1,2\}}^3-32\eta^2\tau\epsilon\varrho_{\{1,1\}}\varrho_{\{1,4\}}\varrho_{\{2,4\}}^3\varrho_{\{2,5\}}^2\varrho_{\{1,2\}}^2\\
&-12\eta^2\tau\epsilon\varrho_{\{1,1\}}^2\varrho_{\{1,4\}}^2\varrho_{\{2,4\}}^2\varrho_{\{2,5\}}^2\varrho_{\{1,2\}}-16\eta\tau^2\epsilon\vartheta_4^2\varrho_{\{2,4\}}^2\varrho_{\{2,5\}}^2\varrho_{\{1,2\}}^3\\
&-16\eta\tau^2\epsilon\vartheta_4\varrho_{\{1,5\}}\varrho_{\{2,3\}}\varrho_{\{2,4\}}\varrho_{\{2,5\}}\varrho_{\{1,2\}}^3-8\eta\tau^2\epsilon\vartheta_4^2\varrho_{\{1,1\}}\varrho_{\{1,4\}}\varrho_{\{2,4\}}\varrho_{\{2,5\}}^2\varrho_{\{1,2\}}^2\\
&-4\eta\tau^2\epsilon\vartheta_4\varrho_{\{1,1\}}\varrho_{\{1,4\}}\varrho_{\{1,5\}}\varrho_{\{2,3\}}\varrho_{\{2,5\}}\varrho_{\{1,2\}}^2-4\eta\tau^2\epsilon\vartheta_4\varrho_{\{1,1\}}\varrho_{\{1,3\}}\varrho_{\{1,5\}}\varrho_{\{2,4\}}\varrho_{\{2,5\}}\varrho_{\{1,2\}}^2\\
&-4\eta\tau^2\epsilon\varrho_{\{1,5\}}^2\varrho_{\{2,3\}}^2\varrho_{\{1,2\}}^3-2\eta\tau^2\epsilon\varrho_{\{1,1\}}\varrho_{\{1,3\}}\varrho_{\{1,5\}}^2\varrho_{\{2,3\}}\varrho_{\{1,2\}}^2\\
&+4\tau^2\vartheta_4\varrho_{\{2,2\}}^2\varrho_{\{2,4\}}\varrho_{\{2,5\}}+2\tau^2\varrho_{\{1,5\}}\varrho_{\{2,2\}}^2\varrho_{\{2,3\}}=0,\\
&-96\gamma c_0\tau^4\vartheta_4\varrho_{\{2,4\}}\varrho_{\{2,5\}}\varrho_{\{1,2\}}^4-48\gamma c_0\tau^4\varrho_{\{1,5\}}\varrho_{\{2,3\}}\varrho_{\{1,2\}}^4-28\eta\tau^2\epsilon\varrho_{\{2,4\}}^4\varrho_{\{2,5\}}^2\varrho_{\{1,2\}}^3-20\eta\tau^2\epsilon\varrho_{\{1,1\}}\varrho_{\{1,4\}}\varrho_{\{2,4\}}^3\varrho_{\{2,5\}}^2\varrho_{\{1,2\}}^2\\
&-8\tau^3\epsilon\vartheta_4^2\varrho_{\{2,4\}}^2\varrho_{\{2,5\}}^2\varrho_{\{1,2\}}^3-8\tau^3\epsilon\vartheta_4\varrho_{\{1,5\}}\varrho_{\{2,3\}}\varrho_{\{2,4\}}\varrho_{\{2,5\}}\varrho_{\{1,2\}}^3-2\tau^3\epsilon\varrho_{\{1,5\}}^2\varrho_{\{2,3\}}^2\varrho_{\{1,2\}}^3=0.
\end{aligned}
$$